QIBA Profile:
Magnetic Resonance Diffusion-Weighted Imaging (DWI) of the Apparent Diffusion Coefficient (ADC)

Table of Contents

1. Executive Summary

The goal of a QIBA Profile is to help achieve a useful level of performance for a given biomarker. The **Claim** (Section 2) describes the biomarker performance and is derived from the body of scientific literature meeting specific requirements, in particular test-retest studies. The **Activities** (Section 3) contribute to generating the biomarker. Requirements are placed on the **Actors** that participate in those activities as necessary to achieve the Claim. **Assessment Procedures** (Section 4) for evaluating specific requirements are defined as needed to ensure acceptable performance.

Diffusion-Weighted Imaging (DWI) and the Apparent Diffusion Coefficient (ADC) are being used clinically as qualitative (DWI) and quantitative (ADC) indicators of disease presence, progression or response to treatment [1-29]. Use of ADC as a robust quantitative biomarker with finite confidence intervals places additional requirements on Sites, Acquisition Devices and Protocols, Field Engineers, Scanner Operators (MR Technologists, Radiologists, Physicists and other Scientists), Image Analysts, Reconstruction Software and Image Analysis Tools [30-37]. Additionally, due to the intrinsic dependence of measured ADC values on biophysical tissue properties, both the Profile Claims and the associated scan protocols (Section 3.6.2) are organ-specific. All of these are considered **Actors** involved in **Activities** of Acquisition Device Pre-delivery and Installation, Subject Handling, Image Data Acquisition, Reconstruction, Registration, ADC map generation, Quality Assurance (QA), Distribution, Analysis, and Interpretation. The requirements addressed in this Profile are focused on achieving ADC values with minimal systematic bias and measurement variability [34, 36, 37].

DISCLAIMER: Technical performance of the MRI system can be assessed using a phantom having known diffusion properties, such as the QIBA DWI phantom. The clinical performance target is to achieve a 95% confidence interval for measurement of ADC with a variable precision depending on the organ being imaged and assuming adequate technical performance requirements are met. While in vivo DWI/ADC measurements have been performed throughout the human body, this Profile focused on four organ systems, namely brain, liver, prostate, and breast as having high clinical utilization of ADC with a sufficient level of statistical evidence to support the Profile Claims derived from the current peer-reviewed literature. In due time, new DWI technologies with proven greater performance levels, as well as more organ systems will be incorporated in future Profiles.

This document is intended to help a variety of users: clinicians using this biomarker to aid patient management; imaging staff generating this biomarker; MRI system architects developing related products; purchasers of such products; and investigators designing clinical trials utilizing quantitative diffusion-based imaging endpoints.

Note that this document only states requirements specific to DWI to achieve the claim, not requirements that pertain to clinical standard of care. Conforming to this Profile is secondary to proper patient care.

2. Clinical Context and Claims

2.1 Clinical Context

The goal of this profile is to facilitate appropriate use of quantitative diffusion weighted imaging (DWI) to gain insight into changes in the microstructure and composition of lesions in humans using precise quantitative measurements of the apparent diffusion coefficient (ADC) for robust tissue characterization and longitudinal tumor monitoring. The premise for its use is that therapy-induced cellular changes should pre-date macroscopic lesion size change, thereby motivating exploration of ADC as a response biomarker [3, 5, 6, 13, 14, 16, 18, 19, 22, 26, 27, 38-40]. Within days to weeks after initiation of effective cytotoxic therapy, tumor necrosis occurs, with a loss of cell membrane integrity and an increase of the extracellular space typically resulting in a relative increase in ADC. During the following weeks to months, the tumor may show shrinkage with a resorption of the free extracellular fluid and fibrotic conversion leading to a decrease of the ADC, although tumor recurrence can also result in reduced ADC [21, 41, 42]. ADC may also change in response to edema, apoptosis, or the use of cytostatic agents.[21, 43]

The objective of this Profile is to provide prerequisite knowledge of the expected level of variance in ADC measurement unrelated to treatment to properly interpret observed change in ADC following treatment [30, 34, 36].

This QIBA DWI Profile makes Claims about the confidence with which ADC values and changes in a lesion can be measured under a set of defined image acquisition, processing, and analysis conditions. It also provides specifications that may be adopted by users and equipment developers to meet targeted levels of clinical performance in identified settings. The intended audience of this document includes healthcare professionals and all other stakeholders invested in the use of quantitative diffusion biomarkers for treatment response and monitoring, including but not limited to:

- Radiologists, technologists, and physicists designing protocols for ADC measurement
- Radiologists, technologists, physicists, and administrators at healthcare institutions considering specifications for procuring new MR equipment
- Technical staff of software and device manufacturers who create products for this purpose
- Biopharmaceutical companies and clinical trialists
- Clinicians engaged in therapy response monitoring
- Radiologists and other health care providers making quantitative measurements on ADC maps
- Oncologists, urologists, neurologists, other clinicians, regulators, professional societies, and others making decisions based on quantitative diffusion image measurements
- Radiologists, health care providers, administrators and government officials developing and implementing policies for brain, liver, prostate, and breast cancer treatment and monitoring

2.2 Claims

Conformance to this Profile <u>by all relevant staff and equipment</u> supports the following claim(s):

Claim 1a: A measured change in the ADC of a brain lesion of 11% or larger indicates that a true change has occurred with 95% confidence.

Claim 2a: A measured change in the ADC of a liver lesion of 26% or larger indicates that a true change has occurred with 95% confidence.

Claim 3a: A measured change in the ADC of a prostate lesion of 47% or larger indicates that a true change has occurred with 95% confidence.

Claim 4a: A measured change in the ADC of a breast lesion of 13% or larger indicates that a true change has occurred with 95% confidence.

Claim 1b: A 95% CI for the true change in ADC of a brain lesion is given below, where Y_1 and Y_2 are the ADC measurements at the two time points:

$$(Y_2 - Y_1) \pm 1.96 \times \sqrt{(Y_1 \times 0.040)^2 + (Y_2 \times 0.040)^2}.$$

Claim 2b: A 95% CI for the true change in ADC of a liver lesion is given below, where Y_1 and Y_2 are the ADC measurements at the two time points:

$$(Y_2 - Y_1) \pm 1.96 \times \sqrt{(Y_1 \times 0.094)^2 + (Y_2 \times 0.094)^2}.$$

Claim 3b: A 95% CI for the true change in ADC of a prostate lesion is given below, where Y_1 and Y_2 are the ADC measurements at the two time points:

$$(Y_2 - Y_1) \pm 1.96 \times \sqrt{(Y_1 \times 0.17)^2 + (Y_2 \times 0.17)^2}.$$

Claim 4b: A 95% CI for the true change in ADC of a breast lesion is given below, where Y_1 and Y_2 are the ADC measurements at the two time points:

$$(Y_2 - Y_1) \pm 1.96 \times \sqrt{(Y_1 \times 0.048)^2 + (Y_2 \times 0.048)^2}.$$

These claims hold when:

- The same imaging methods on the same scanner and the same analysis methods are used at two separate time points where the interval between measurements is intended to represent the evolution of the tissue over the interval of interest (such as pre-therapy versus post initiation of therapy).
- Conspicuity of lesion boundary is adequate to localize the lesion for definition on a region-of-interest [27] at both time points.
- For breast, a whole lesion/tissue (multi-slice) ROI is used [44, 45] at each timepoint.

Discussion

- These claims are based on estimates of the within-subject coefficient of variation (wCV) for ROIs drawn in the brain, liver, prostate, and breast. For estimating the critical % change, the % Repeatability Coefficient (%RC) is used: 2.77 × wCV × 100%, or %RC = 11% for brain, 26% for liver, 47% for prostate, and 13% for breast. Specifically, it is assumed that the wCV is 4% for brain, 9.4% for liver, 17% for prostate, and 4.8% for the breast. The claim assumes that the wCV is constant for tissue regions in the specified size, the signal-to-noise ratio (SNR) of the tissue region

on the *b*=0 image is at least 50, and that the measured ADC is linear (slope=1) with respect to the true ADC value over the tissue-specific range $0.3x10^{-3}$ mm^2/s to $3.0x10^{-3}$ mm^2/s.

- For the brain, estimates are from Bonekamp 2007, Pfefferbaum 2003 (mean ADC in an anatomical region or polygonal ROI), and Paldino 2009 [46-48]; for the liver, estimates are from Miquel 2012, Braithwaite 2009 (mean ADC in an ROI between 1-4 cm^2) [49-52]; for the prostate, estimates are from Litjens 2012, Fedorov 2017 and Gibbs 2007 (Table 1 of the manuscript, mean ADC is from an ROI ranging from 120 to 320 mm^2, with little impact on repeatability) [53-57]. The claims of this Profile, informed by this cited literature, do not address heterogeneity in prostate; zone-specific ROIs may result in lower wCVs. For the breast, estimates are for mean ADC in a multi-slice ROI from Newitt 2018 [44] (covering the whole tumor)) and Sorace 2018 [45] (normal breast fibroglandular tissue).
- In general, where there is test-retest data for ADC, there is usually not consistent accompanying information about ROI size and shape. It will be valuable to have such information to better inform future claim statements.

2.3 Clinical Interpretation

In tumors, changes in ADC can reflect variations in cellularity, as inferred by local tissue water mobility, e.g., a reduction or increase of the extracellular space, although the level of measured change must be interpreted relative to the Repeatability Coefficient before considered as a true change [1, 30, 34, 37, 44-49, 52, 57-59]. Other biological processes may also lead to changes in ADC, e.g., stroke.

Low ADC values suggest cellular dense tissue and potentially solid/viable tumor as opposed to elevated ADC values in tumor necrosis and cystic spaces. For example, ADC in the peripheral zone of the prostate decreases with the presence of cancer (while generally increasing with age) [60]. Care should be taken to correlate ADC findings with morphology, e.g., with T_2-weighted images in the prostate in the case of an abscess. The use of specific interpretation of ADC values will depend on the clinical application, e.g., considering spontaneous tumor necrosis versus tumor necrosis after effective therapy. Schema and properties of tissues to assay by ADC should be addressed during the design phase of each study. For example, therapies targeted to induce cytotoxic change in solid viable tumor [3, 19, 22, 38, 41] are candidate for ADC monitoring by ROI segmentation guided by traditional MR indicators of solid viable tissue, namely: relatively hyperintense on high *b*-value DWI, low ADC, and perfused on dynamic contrast-enhanced MRI. The anticipated timescale of ***early*** therapeutic response and/or tumor progression must be considered in study design of MRI scan dates for application of ADC as a prognostic marker.

3. Profile Activities

The Profile is documented in terms of "Actors" performing "Activities". Equipment, software, staff or sites may claim conformance to this Profile as one or more of the "Actors" in the following table.

Conformant Actors shall support the listed Activities by conforming to all requirements in the referenced Section.

For some activity parameters, three specifications have been defined. Meeting the ACCEPTABLE specification is sufficient to conform to the profile. Meeting the TARGET or IDEAL specifications is expected to achieve improved performance but are not required for conformance to the profile.

ACCEPTABLE: Actors that shall meet this specification to conform to this profile.

TARGET: Meeting this specification is achievable with reasonable effort and adequate equipment and is expected to provide better results than meeting the ACCEPTABLE specification.

IDEAL: Meeting this specification may require extra effort or non-standard hardware or software, but is expected to provide better results than meeting the TARGET.

Table 1: Actors and Required Activities

Actor (Checklist Appendix)	Activity	Section
Site (see F.1)	Qualification and Periodic QA	3.2, 3.5
Acquisition Device (see F.2)	Site Qualification	3.2
	Protocol Design	3.6
	Image Distribution	3.12
Scanner Operator* (see F.3)	Site Qualification	3.2
	Image Data Reconstruction	3.10
Image Analyst† (see F.4)	Staff and Site Qualification	3.1 and 3.2
	Image Analysis	3.13
Reconstruction Software (see F.5)	Image Data Reconstruction	3.10
Image Analysis Tool (see F.6)	Image Analysis	3.13

*Scanner operator may be an MR technologist, physicist, or other scientist
†Image analyst may be a radiologist, technologist, physicist, or other scientist.

The requirements in this Profile do not codify a Standard of Care; they only provide guidance intended to achieve the stated Claim. Failing to conform to a "shall" statement in this Profile is a protocol deviation. Handling protocol deviations for specific trials/studies is at full discretion of the study sponsors and other responsible parties.

Example of a clinical trial workflow based on this DWI Profile is shown in Figure 1:

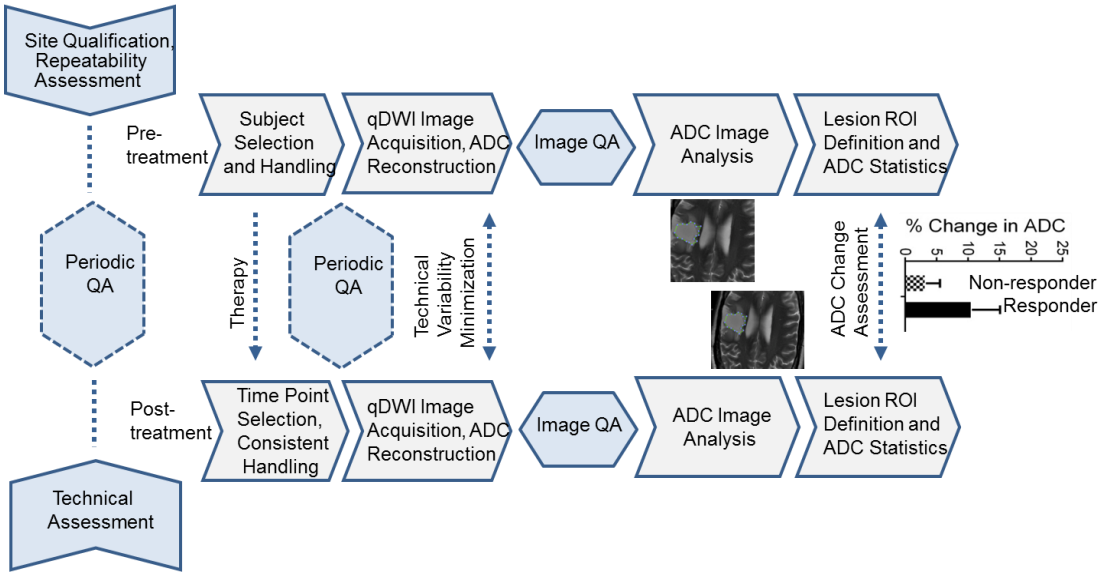

Figure 1: Typical quantitative Diffusion-Weighted MRI trial workflow for Treatment Response Assessment with key QIBA profile activities

3.1. Staff Qualification

This activity involves evaluating the human Actors (Radiologist, Scanner Operator and Image Analyst) prior to their participation in the Profile.

3.1.1 Discussion

These requirements, as with any QIBA Profile requirements, are focused on DWI-relevant activities required to achieve the DWI Profile Claims. Evaluating the medical or professional qualifications of participating actors is beyond the scope of this profile.

In clinical practice, it is expected that the radiologist interpreting the examination often will be the image analyst. In some clinical practice situations, and in the clinical research setting, the image analyst may be a non-radiologist professional such as a medical physicist, biomedical engineer, MRI scientist or 3D lab technician. While there are currently no specific certification guidelines for image analysts, a non-radiologist performing diffusion analysis should be trained in technical aspects of DWI including: understanding key acquisition principles of diffusion weighting and directionality and diffusion test procedures (Appendix E); procedures to confirm that diffusion-related DICOM metadata content is maintained along the network chain from scanner to PACS and analysis workstation. The analyst must be

expert in use of the image analysis software environment, including ADC map generation from DWI (if not generated on the scanner), and ADC map reduction to statistics with ROI/VOI location(s) retained. The analyst should undergo documented training by a radiologist having qualifications conforming to the requirements of this profile in terms of anatomical location and image contrast(s) used to select measurement target. The level of training should be appropriate for the setting and the purpose of the measurements. It may include instruction in topics such as directional and isotropic DWI and ADC map reconstruction and processing; normative ADC values for select tissues; and recognition of image artifacts. The Technologist is always assumed to be a Scanner Operator for subject scanning, while phantom scanning can be performed by the Image Analyst.
http://www.acraccreditation.org/~/media/ACRAccreditation/Documents/MRI/Requirements.pdf?la=en

3.1.2 SPECIFICATION

Parameter	Actor	Specification
Qualification	Image Analyst	Shall be a radiologist, technologist, physicist, or other scientist with documented and authorized training in terms of: anatomical location and image contrast(s) used to select measurement target; understanding key principles of diffusion weighting, directionality, and diffusion test procedures; procedures to maintain diffusion-related DICOM metadata content along the network chain from Scanner to PACS and analysis workstation; the use of the Image Analysis Tool, including ADC map generation from DWI (if not generated on the scanner), and ADC map reduction to statistics with ROI/VOI location(s)

3.2. Site qualification

This activity involves evaluating performance of the product Actors (Acquisition Device, Reconstruction Software, and Image Analysis Tool) by the Scanner Operator and Image Analyst initially at the site to ensure acceptance to the trial and baseline cross-site protocol standardization, but not directly associated with a specific clinical trial subject, that are necessary to reliably meet the Profile Claim.

3.2.1 DISCUSSION

Site qualification testing will be performed according to the trial-specific multi-site protocol prior to inclusion into trial to check site's ability to implement standardized acquisition protocol and image analysis, as well as establish the baseline performance level. Steps toward multi-device standardization include meeting the baseline performance specifications for bias and repeatability using quantitative DWI phantom [61-63]. The listed specifications are based on the prior multi-system studies [62, 64-67]. The details on the platform-specific phantom scanning protocols and performance metrics assessment are provided in Section 4 and Appendices D and E.

Key quantitative DWI performance metrics include: ADC bias at magnet isocenter, random error within ROI (precision), SNR at each *b*-value, ADC dependence on *b*-value and ADC spatial dependence. To conform to this Profile, system performance benchmarks for these metrics are provided in 3.2.2 to ensure negligible contribution of technical errors to above defined confidence intervals measured for tissue. These benchmarks reflect the baseline MRI equipment performance in clinical and multi-center clinical trial settings to support the Claims of this Profile. To establish tighter confidence bounds for ADC metrics, additional technical assessment procedures may be introduced according to specific clinical trial protocol. Note that with other performance assessment metrics conformant to the Profile, the listed acceptable ranges

for spatial ADC bias could be the major source of the technical measurement error limiting ADC confidence intervals in multi-center studies.

3.2.2 SPECIFICATION

Parameter	Actor	Requirement
Qualification activities	Site	Shall perform qualification activities for Acquisition Device, Scanner Operator, and Image Analyst to meet equipment, reconstruction SW, image analysis tool and phantom ADC performance metrics as specified in Table 3.2.2 and by trial-specific protocol 3.6.2
Acquisition Protocols	Scanner Operator	Shall prepare scan protocols conformant with section 3.6.2 "Protocol Design Specification" and phantom qualification (Appendix D) and ensure that DWI acquisition parameters (*b*-value, diffusion direction) shall be preserved in DICOM and shall be within ranges allowed by study protocol (both for phantom and subject scans). Shall check for protocol conformance, consistent patient positioning (orientation, target lesion location relative to isocenter), and that all subject-specific adjustments (i.e., to suit body habitus) are consistent across serial scans.
Acquisition Device Performance		Shall perform assessment procedures (Section 4) for site qualification and longitudinal QA for the acquisition devices participating in trial to document acceptable performance for phantom ADC metrics as specified in table 3.2.2
Acquisition Device		The same scanner shall be used for baseline and subsequent longitudinal measurements for detecting change in ADC.†
Image Analysis Tool Performance	Image Analyst	Shall test Image Analysis Tool to ensure acceptable performance according to 3.13.2 specifications for study image visualization, DICOM and analysis meta-data interpretation and storage, ROI segmentation, and generation of ADC maps and repeatability statistics for qualification phantom (below)
Phantom ADC ROI		Shall confirm that phantom ADC ROI is 1–2 cm diameter (< 80 pixels without interpolation) for all Acquisition Device specifications in Table 3.2.2
Phantom ADC metrics		Shall evaluate and record phantom ADC metrics (bias, linearity and precision) according to Table 3.2.2 specifications for Acquisition Device qualification and periodic QA using QIBA-provided or qualified site Image Analysis Tool, or QIBA-certified 3rd party analysis services
DWI Tags	Acquisition Device	Shall preserve tags related to DWI, including private tags, which may be vendor-specific. Some key tags are specified in Appendix D.
Short-term (intra-exam) ADC repeatability at/near isocenter		RC $\leq 1.5 \times 10^{-5}$ mm^2/s and wCV $\leq 0.5\%$ for ice-water phantom or other quantitative DWI phantom

Parameter	Actor	Requirement
Long-term (multi-day) ADC repeatability at/near isocenter		RC ≤ $6.5x10^{-5}$ mm^2/s and wCV ≤ 2.2% for ice-water phantom or other quantitative DWI phantom
DWI *b*=0 SNR		SNR (*b*=0) ≥ 50 ± 5 for ice-water phantom or other quantitative DWI phantom.
ADC *b*-value dependence		< 2% for ice-water phantom or other quantitative DWI phantom over *b*-value pairs 0-500; 0-1000; 0-1500; and 0-2000 s/mm^2
Maximum |bias| with offset from isocenter, within 4 cm in any direction		< 4% for uniform known ADCs within DWI phantom
ADC error at/near isocenter		ADC random error ≤ 2% for ice-water phantom or other quantitative DWI phantom
Optional: Additional requirements for studies involving off-center ADC measurement:		
R/L offset 4–10 cm (A/P, S/I < 4 cm)	Acquisition Device	< 10% for uniform known ADCs within DWI phantom
A/P offset 4–10 cm (R/L, S/I < 4 cm)		< 10% for uniform known ADCs within DWI phantom
S/I offset 4–10 cm (R/L, A/P < 4 cm)		< 10% for uniform known ADCs within DWI phantom

† Not using the same scanner and image acquisition parameters for baseline and subsequent measurements does not preclude clinical use of the measurement but will exclude meeting the requirements of the Profile claim.

3.3. Pre-delivery

Standard scanner calibrations, phantom imaging, performance assessments or validations prior to delivery of equipment to a site (e.g., performed at the factory) for routine clinical service are beyond the scope of this profile but are assumed to be satisfied.

3.3.1 Discussion

Current clinical MR scanners equipped with single-shot echo planar DWI capabilities compliant with trial acquisition protocol are adequate to meet the Profile Claim.

3.4. Installation

Beyond standard installation activities which are outside the scope of this profile, network DICOM client configuration of PACS and analysis workstation(s) shall maintain all DWI-relevant DICOM metadata.

3.5. Periodic QA

This activity describes phantom imaging, performance assessments or validations performed after initial acceptance to the trial and periodically at the site, but not directly associated with a specific subject, that are necessary to reliably meet the Profile Claim.

3.5.1 DISCUSSION

Periodic quality assurance procedures should be consistent with those generally accepted for routine clinical imaging but are outside the scope of this profile. Additional DWI-specific QA procedures to ensure baseline scanner performance with minimal technical variability are described in Section 4 and Appendices D and E and can be utilized as needed [21, 68]. Presently, there are insufficient data to require a set frequency of periodic QA, which is specific to the clinical trial design. However, QA procedures should be followed after a hardware or software upgrade.

3.5.2 SPECIFICATION

Parameter	Actor	Requirement
Periodic DWI QA	Site	Shall perform annual periodic QA (and after major hardware or software changes) for Acquisition Device that includes assessment of ADC bias, random error, linearity, DWI SNR, DWI image artifacts, *b*-value dependence (linearity) and spatial uniformity (3.2.2)
Equipment	Site	Same, pre-qualified equipment and SW shall be used over the length of trial, and all preventive maintenance shall be documented over the course of the trial. Re-qualification shall be performed in case of major SW or hardware upgrade. Study of each patient shall be performed on the site pre-qualified scanner using approved receiver coil and pre-built profile-conformant scan protocol (3.6)

3.6. Protocol Design

This activity involves designing DWI acquisition and reconstruction procedures that are necessary to reliably meet the Profile Claim. Along with site qualification (3.2), this activity facilitates cross-platform protocol standardization for multi-site trials.

3.6.1 DISCUSSION

The Profile considers Protocol Design to take place at the imaging site, however, sites may choose to make use of protocols developed elsewhere. DWI scan protocols (for phantom QA and subject scanning) should be pre-built by the Scanner Operator during site qualification (3.2.2), clearly labeled and stored on the MRI system for recall in study scans with minimal parameter changes within allowed specification ranges. Version control of edits to the protocol should be tracked with prior versions archived. Standardized DWI phantom scan protocols are tabulated in Appendix D.

Tables in section 3.6.2 contain key specifications for subject DWI scan protocols expressed using generic terminology. The specifications are consistent with publications supporting Profile Claims and consensus recommendations for brain [31, 46-48, 69], liver [21, 28, 49-52, 59] and prostate [53-57, 60]. Some parameters include a numerical range. Reduction of respiratory artifact in the liver requires either short breath-hold (un-averaged, < 25 sec), or long (3-5 min) respiratory-synchronization, or free breathing with high signal averaging. The gain in image quality with high signal averaging favors use of non-breath-hold abdominal DWI. New techniques, such as simultaneous multi-slice or multi-band MRI, are becoming commercially available and could be advantageous for DWI [70-73]. *k*-space undersampling, rFOV, and multi-shot EPI techniques are also becoming more common [74-80]. However, these are not yet considered "standard" on most clinical systems and therefore are not specified below. The literature which informs the prostate claim in Section 2 presents 3T data with body coil exclusively; therefore, the associated prostate

protocols in this Profile are limited to 3T. This Profile does not yet address the use of DWI at high (> 3 T) or low-field (< 1.5 T) strengths due to the absence of test-retest literature.

Care should be taken to utilize the same scan parameters across exams, particularly within a study. For example, close attention should be paid to the TE, which should be consistent across exams.

In the specification tables, there are requirements to include b=0 s/mm^2 images. This hastens image acquisition by obviating acquisition of multiple directions to enable directional averaging of non-zero b-values, however low. However, some scanners do not produce a "true-zero" b-value. Whenever possible, true-zero b-value should be acquired; when hardware or software makes this not possible, $b < 50$ s/mm^2 can be acquired in lieu of true-zero b-values.

In the case of breast imaging (3.6.2.4), phase encoding along the anterior-posterior axis preserves anatomic symmetry for axial breast fields of view, and is preferred over left-right phase encoding (which is still acceptable).

3.6.2 SPECIFICATION

Parameter	Actor	Requirement
Scan Protocol Parameters, DICOM Conformance, and Image Reconstruction	Acquisition Device	Device scan protocol parameters shall be within organ-specific ranges listed in the protocol specification tables (3.6.2). Shall be capable of performing reconstructions and producing images with all the parameters set as specified. Shall meet DICOM header and image registration requirements specified in 3.10.2, including storage of b-values, DWI directionality, image scaling and units tags, as specified in DICOM conformance statement for the given scanner SW version, as well as the model-specific Reconstruction Software parameters utilized to achieve conformance.

3.6.2.1 Brain

Parameter	Actor	Requirement	DICOM Tag†
Field Strength	Scanner Operator	1.5 or 3T	[0018, 0087]
Acquisition sequence		Diffusion-weighted Single-Shot Echo Planar Imaging (SS-EPI)	[0018, 0020]
Receive Coil type		Ideal: 32 channel head array coil Target: 8–32 channel head array coil Acceptable: 8 channel head array coil	[0018, 1250]
Lipid suppression		On	

Number of *b*-values		Ideal: ≥ 3 (including one *b*=0–50; one 450–550 s/mm^2; and one at highest *b*-value) Acceptable/Target: 2 (including *b*=0–50 s/mm^2 and at highest *b*-value)	
Minimum highest *b*-value		Target/Ideal: *b*=1000 s/mm^2 Acceptable: *b*=850–999 s/mm^2	[0018, 9087]
Diffusion directions		Target/Ideal: ≥ 3-orthogonal, combined gradient channels	[0018, 9075]
		Acceptable: ≥ 3-orthogonal, single gradient channels	[0018, 9089]
Slice thickness		Ideal: ≤ 4 mm Target: 4–5 mm Acceptable: 5 mm	[0018, 0050]
Gap thickness		Target/Ideal: 0–1 mm Acceptable: 1–2 mm	[0018, 0088]
Field-of-view		220–240 mm FOV along both axes	[0018, 1100]
Acquisition matrix		Target/Ideal: (160–256) x (160–256), or 1.5–1 mm in-plane resolution Acceptable: 128 x 128, or 1.7 mm in-plane resolution	[0018, 1310]
Plane orientation		Transversal-axial	[0020, 0037]
Phase-encode/ frequency-encode direction		Anterior-Posterior / Right-Left	[0018, 1312]
Number of averages		Ideal/Target: ≥ 2 Acceptable: 1	[0018, 0083]
Half-scan factor		Acceptable/Target: > 0.65	[0018, 9081]
In-plane parallel imaging acceleration factor		Ideal: 2–3 Acceptable/Target: 2	[0018, 9069]
TR		Ideal: > 5000 ms Acceptable/Target: 3000–5000 ms	[0018, 0080]
TE		Ideal: < 60 ms Target: minimum TE Acceptable: < 120 ms	[0018, 0081]
Receiver Bandwidth		Ideal/Target: maximum possible in frequency encoding direction (minimum echo spacing) Acceptable: > 1000 Hz/voxel	[0018, 0095]

3.6.2.2 Liver

Parameter	Actor	Requirement	DICOM Tag[†]
Field Strength	Scanner Operator	1.5 or 3 T	[0018, 0087]
Acquisition sequence		Diffusion-weighted Single-Shot Echo Planar Imaging (SS-EPI)	[0018, 0020]
Receive Coil type		Ideal: >16 channel torso array coil Target: 6–16 channel torso array coil Acceptable: 6 channel torso array coil	[0018, 1250]
Lipid suppression		On	
Number of *b*-values		Ideal: ≥ 3 (including one *b*=0–50; one 100–300 s/mm^2; and one at highest *b*-value) Acceptable/Target: 2 (including one *b*=50–100 s/mm^2 and one at highest *b*-value)	
Minimum highest *b*-value		Target/Ideal: *b*=600–800 s/mm^2 Acceptable: 500 s/mm^2	[0018, 9087]
Diffusion directions		Target/Ideal: 3-orthogonal, combined gradient channels Acceptable: 3-orthogonal, single gradient channels	[0018, 9075] [0018, 9089]
Slice thickness		Ideal: < 5 mm Target: 5–7 mm Acceptable: 7–9 mm	[0018, 0050]
Gap thickness		Ideal: 0 mm Target: 1 mm Acceptable: > 1–2 mm	[0018, 0088]
Field-of-view		300–450 mm	[0018, 1100]
Acquisition matrix		Target/Ideal: (160–196) x (160–192), or 2.5–2 mm in-plane Acceptable: 128 x 128, or 3–2.6 mm in-plane resolution	[0018, 1310]
Plane orientation		Transversal-axial	[0020, 0037]
Half-scan factor		Acceptable/Target: > 0.65	[0018, 9081]
Phase-encode/ frequency-encode direction		Anterior-Posterior / Right-Left	[0018, 1312]
Number of averages		Ideal: > 4 Target: 4 Acceptable: 2–3	[0018, 0083]
Parallel imaging factor		Ideal: 2-3 Target/Acceptable: 2	[0018, 9069]

TR		Ideal/Target/Acceptable: > 2000 ms	[0018, 0080]
TE		Ideal: < 60 ms Target: minimum TE Acceptable: < 110 ms at 1.5T; < 90 ms at 3T	[0018, 0081]
Receiver Bandwidth		Ideal/Target: maximum possible in frequency encoding direction (minimum echo spacing)	[0018, 0095]
		Acceptable: > 1000 Hz/voxel	

3.6.2.3 Prostate

Parameter	**Actor**	**Requirement**‡	**DICOM Tag**†
Field Strength	Scanner Operator	3 T	[0018, 0087]
Acquisition sequence		Diffusion-weighted Single-Shot Echo Planar Imaging (SS-EPI)	[0018,0020]
Receive Coil type		Ideal/Target: ≥ 8 channel torso array coil Acceptable: < 8 channel pelvic phased array coil/endorectal coil; body array coil	[0018,1250]
Lipid suppression		On	
Number of *b*-values‡		Ideal: ≥ 3 (including one *b*=0-50; one 100–500 s/mm^2; and one at highest *b*-value) Acceptable/Target: 2 (including one *b* < 50–100 s/mm^2 and one at highest *b*-value)	
Minimum highest *b*-value‡		Ideal: *b*=1000–1500 s/mm^2 Target/Acceptable: 500–1000 s/mm^2	[0018, 9087]
Diffusion directions		Target/Ideal: 3-orthogonal, combined gradient channels	[0018, 9075]
		Acceptable: 3-orthogonal, single gradient channels	[0018, 9089]
Slice thickness‡		Ideal: ≤ 3 mm Target: 3–4 mm Acceptable: 4–5 mm	[0018, 0050]
Gap thickness		Ideal: 0 mm Target/Acceptable: 1 mm	[0018, 0088]
Field-of-view‡		240–260 mm	[0018, 1100]
Acquisition matrix‡		(224–128) x (224–128), or 2–1 mm in-plane	[0018, 1310]
Plane orientation		Transversal-axial	[0020, 0037]
Half-scan factor		Acceptable/Target: > 0.65	[0018, 9081]
Phase-encode/ frequency-encode direction		Anterior-Posterior / Right-Left	[0018, 1312]

Number of averages		Ideal: > 4 Target: 4 Acceptable: 2–4	[0018, 0083]
Parallel imaging factor		Ideal /Target/Acceptable: 2	[0018, 9069]
TR‡		Ideal/Target/Acceptable: > 2000 ms	[0018, 0080]
TE		Ideal: < 60 ms Target: minimum TE Acceptable: ≤ 90 ms	[0018, 0081]
Receiver Bandwidth		Ideal/Target: maximum possible in frequency encoding direction (minimum echo spacing) Acceptable: > 1000 Hz/voxel	[0018, 0095]

†Only public DICOM tags are listed above. Vendors storing key acquisition meta-data in non-standard (private tags) should provide DICOM conformance statement listing the corresponding header items.
‡PI-RADS recommendations can differ from the protocols derived from the cited literature in this Profile. The PI-RADS v2 recommendations can be found at:
https://www.acr.org/~/media/ACR/Documents/PDF/QualitySafety/Resources/PIRADS/PIRADS%20V2.pdf

3.6.2.4 Breast

Parameter	**Actor**	**Requirement**	**DICOM Tag†**
Field Strength	Scanner Operator	1.5 or 3 T	[0018, 0087]
Acquisition sequence		Diffusion-weighted Single-Shot Echo Planar Imaging (SS-EPI)	[0018, 0020]
Receive Coil type		Ideal/Target: 5–16 channel bilateral breast coil Acceptable: 4 channel bilateral breast coil	[0018, 1250]
Lipid suppression		Ideal/Target: combined spectral and relaxation-based fat suppression (e.g., SPAIR Acceptable: Relaxation-based (STIR) or spectral-based (fat-sat) alone if SPAIR is not available	
Number of *b*-values		Ideal: ≥ 4 Target/Acceptable: 3 (including one *b*=0–50; one 100 s/mm^2; and one at highest *b*-value)	
		Acceptable: 2 (including one *b*=0–50 s/mm^2 and one at highest *b*-value)	

Minimum highest *b*-value		Target/Ideal: *b*=600–800 s/mm^2	[0018, 9087]
		Acceptable: 600 s/mm^2	
Diffusion directions		Target/Ideal: 3-orthogonal, combined gradient channels	[0018, 9075]
		Acceptable: 3-orthogonal, single gradient channels	[0018, 9089]
Slice thickness		Ideal: 4 mm Target: 4–5 mm Acceptable: 5 mm	[0018, 0050]
Gap thickness		Ideal: 0 mm Target: 0–1 mm Acceptable: 1 mm	[0018, 0088]
Field-of-view		Ideal/Target/Acceptable: 260–360 mm *complete bilateral coverage	[0018, 1100]
Acquisition matrix		Target/Ideal: (128–192) x (128–192), or 2.8–1.8 mm in-plane Acceptable: 128 x 128, or 2.8 mm in-plane resolution	[0018, 1310]
Plane orientation		Transversal-axial	[0020, 0037]
Half-scan factor		Acceptable/Target: > 0.65	[0018, 9081]
Phase-encode/ frequency-encode direction		Ideal/Target: Anterior-Posterior/Right-Left Acceptable: Right-Left /Anterior-Posterior	[0018, 1312]
Number of averages		Ideal/Target: 3–5 Acceptable: 2	[0018, 0083]
Parallel imaging factor		Ideal: ≥ 2 Target/Acceptable: 1.5–2	[0018, 9069]
TR		Ideal/Target/Acceptable ≥ 4000 ms	[0018, 0080]
TE		Ideal/Target: minimum TE (50–100 ms) Acceptable: < 114 ms	[0018, 0081]
Receiver Bandwidth		Ideal/Target: maximum possible in frequency encoding direction (minimum echo spacing) Acceptable: > 1000 Hz/voxel	[0018, 0095]

3.7. Subject Selection

This activity describes criteria and procedures related to the selection of appropriate imaging subjects. General MRI subject safety is assumed to be observed, but is beyond the scope of this DWI-specific Profile.

3.7.1 DISCUSSION

Despite having an acceptable risk status, metal-containing implants and devices near the tissue/organ/lesion of interest may introduce artifact and may not be suitable for DWI.

For specific study/trial, subject scan timing should be appropriately synchronized with the assayed subject condition (e.g., clinical state or therapeutic phase) per study design.

3.8. Subject Handling

This activity describes details of handling imaging subjects that are necessary to meet this Profile Claims. General MRI subject safety considerations apply but are beyond the scope of this Profile.

3.8.1 DISCUSSION

Brain, liver, and breast DWI do not require special subject handling. To reduce motion artifact from bowel peristalsis during prostate imaging, the use of an antispasmodic agent may be beneficial in some patients. The presence of air and/or stool in the rectum may induce artifactual distortion that can compromise DWI quality. Thus, some type of minimal preparation enema administered by the patient in the hours prior to the exam maybe beneficial. However, an enema may also promote peristalsis, resulting in increased motion related artifacts in some instances. The patient should evacuate the rectum, if possible, just prior to the MRI exam.

3.9. Image Data Acquisition

This activity describes details of the subject/patient-specific image acquisition process that are necessary to reliably meet the DWI Profile Claim.

3.9.1 DISCUSSION

Starting from the pre-built scan protocol, the technologist (scanner operator) will orient and position receiver coil study subjects uniformly. Patient-size parameter adjustments will be within allowed parameter ranges, and the same adjustments will be used for serial scans of given subject. To reduce spatial bias, when possible, the landmark will be placed close to the center of the target organ (e.g., prostate).

3.10. Image Data Reconstruction

This activity describes criteria and procedures related to producing images from the acquired data that are necessary to reliably meet the DWI Profile Claims.

3.10.1 DISCUSSION

At a minimum, three-orthogonal directional DWI are acquired and reconstructed individually for each imaged slice, then combined into a directionally-independent (i.e. isotropic or trace) DWI [81, 82]. Diffusion weighted images may be interpolated to an image matrix greater than the acquired matrix. Directionally-independent trace or isotropic DWI are often automatically generated and retained by reconstruction software on the scanner for each non-zero *b*-value, whereas retention of directional DWI is optional. ADC maps are typically generated on the scanner using a mono-exponential model trace DWI vs. *b*-value. Alternatively, full DWI sets (directional plus trace, or trace alone) at all *b*-values can be provided for off-line ADC map generation (via mono-exponential model) on an independent workstation or thin-client distributed application.

Eddy currents and/or subject motion may create spatial misalignment or distortion between the individual directional DWI, and across *b*-values [83-85]. Direct combination of misaligned directional DWI will lead to spatial blur in trace DWI and subsequent artifact in ADC maps [83-85]. Spatial registration of directional

DWI and/or trace DWI across all *b*-values may be performed on the scanner or off-line to reduce blur and improve quality of trace DWI and ADC maps.

Perfusion is known to affect diffusion measurement (a positive bias) particularly in highly vascular tissues (e.g., kidney and liver) [86-91]. ADC values derived from DWI spanning low *b*-value (i.e., $b < 50 s/mm^2$) and modest high *b*-value (i.e., $b < 500$ s/mm^2) increase perfusion bias. For diffusion measurement in liver, ADC maps should be reconstructed from DWI spanning 50-100 s/mm^2 up to 800-900 s/mm^2 to mitigate perfusion bias while maintaining adequate sensitivity to diffusion contrast and SNR. The degree of potential perfusion contamination of ADC will depend on blood volume fraction, number and distribution of *b*-values. Perfusion bias in brain DWI is considered small and typically ignored. There is a small deviation from mono-exponential decay (pseudo-diffusion) at low *b*-values in prostate [92].

3.10.2 SPECIFICATION

Parameter	Actor	Requirement
Trace DWI and ADC map generation across subjects and time	Scanner Operator	Number and magnitude of *b*-values shall be consistent across TPs for patients. ADC maps shall be generated in a consistent manner across TPs, including post-processing, fit model, and image registration.
b-value record		Scanner operator shall verify that the reconstruction SW records *b*-values, or if not shall manually record the *b*-values, that are used to generate the ADC map.
ADC maps		ADC maps shall be preserved with DICOM scale tags. ADC map scale/units and *b*-values used for generation shall be recorded.
Trace DWI	Reconstruction Software	Trace DWI shall be auto-generated on the scanner and retained for all $b > 0$. For equal *b*-value on 3 orthogonal directions, trace DWI is the geometric average of the 3-orthogonal directional DWI.

3.11. Image QA

This activity describes criteria and evaluations of the images necessary to reliably meet the Profile Claim.

3.11.1 DISCUSSION

At the time of image acquisition and review, quality of DWI data should be checked for the following issues. Poor quality due to sources below may be grounds to reject individual datasets:

- Low SNR – Diffusion weighting inherently reduces signal, although signal must remain adequately above the noise floor to properly estimate ADC [93-95]. In general, the SNR at b=0 s/mm^2 should be greater than 50. Low SNR (< 5) at high *b*-values can bias ADC estimates. Visualization of anatomical features in tissues of interest at all *b*-values is acceptable evidence that SNR is adequate for ADC measurement (Figure 2 and Figure 3). Appendix E.2 provides instructions for measuring SNR in diffusion-weighted imaging, as well as guidance for the use of an appropriate DRO.
- Ghost/parallel imaging artifacts – Discrete ghosts from extraneous signal sources along phase-encode direction can obscure tissue of interest leading to unpredictable ADC values [84, 96-101] (Figure 2d, Figure 4, and Figure 8a).

- Severe spatial distortion – Some level of spatial distortion is inherent to SS-EPI, although distortion can be severe near high susceptibility gradients in tissues or metallic objects (Figure 3b, Figure 8c); or due to poor magnet homogeneity [84, 98]. Severe distortion can alter apparent size/shape/volume of tissues of interest thereby confound ROI definition, as well as adversely affect ADC values. Co-registration to high-resolution (non-EPI) T2-weighted image volume may reduce these distortions.

- Eddy currents – Distinct eddy currents amplified by strong diffusion pulses on different gradient channels lead to spatial misalignment across acquired DWI directions and *b*-values, and are manifest as spatial blur on trace DWI and erroneous ADC values particularly at the edges of anatomical features [84, 102] (Figure 5, Figure 9). Distortion correction and image registration to b=0 image prior to calculation of trace DWI and ADC maps may reduce these errors. Further artifact mitigation may be achieved by the use of double-spin echo bipolar-gradient pulse sequences, in particular at high *b*-values.

- Fat suppression – Lipid exhibits extremely low diffusion, with fat spatially shifted on SS-EPI from its true source (by several cm along the phase-encode direction) due to chemical shift [103-107]. Of note, scanner frequency drifting due to the heating from high duty cycle diffusion gradients could cause unsatisfactory fat suppression in the later frames of a diffusion acquisition, if only chemical shift saturation technique is used for fat suppression. In such case, alternative or additional fat suppression techniques, e.g., gradient reversal, could help to mitigate residual fat signal. Superposition of unsuppressed fat signal onto tissue of interest (Figure 6, Figure 8b) can invalidate ADC assessment there by partial volume averaging.

- Motion artifacts — While SS-EPI is effective at freezing most bulk motion, variability of motion over DWI directions and *b*-values contribute to blur and erroneous signal attenuation. Motion artifact is anticipated to be low in brain DWI for most subjects, although cardiac-induced pulsation can confound ADC measurement in/near ventricles and large vessels and in the brainstem. Respiratory and cardiac motion artifacts are more problematic in the liver, particularly the left-lobe and superior right lobe [12, 28, 98, 108, 109]. Quiet steady breathing or respiratory synchronization and additional signal averaging are used to mitigate motion artifact in abdominal DWI. Residual motion artifact can be recognized as inconsistent location of anatomical targets across *b*-values and DWI directions and/or spatial modulation unrelated to anatomical features on DWI/ADC maps. Inspection of DWI/ADC on orthogonal multi-planar reformat images aids detection of this artifact (Figure 7). Anti-peristaltic drugs and voiding of the rectum reduce motion- and susceptibility-induced artifacts when imaging the prostate, respectively.

- Nyquist ghost – EPI sequences acquire data using alternating readout gradient polarity between odd and even *k*-space lines. The associated eddy currents and resultant magnetic fields produce inconsistent phase shifts between even and odd echoes resulting in ghost artifacts that are referred to as Nyquist or N/2 ghosts (Figure 8a). Use of parallel imaging techniques results in additional copies of the N/2 ghost [101, 110].

Examples of common artifacts that may affect ADC maps are provided below:

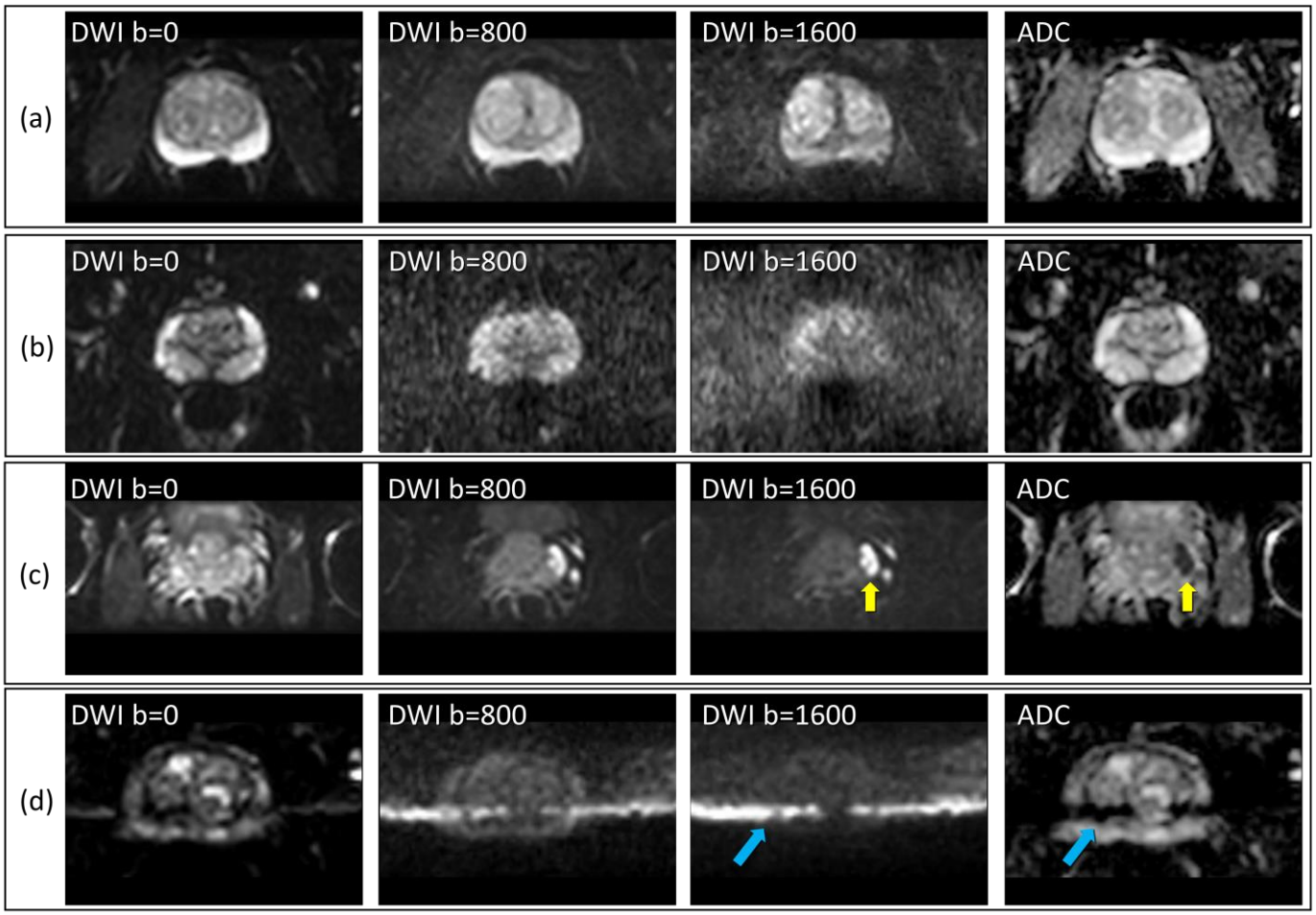

Figure 2: Visual assessment of SNR in prostate DWI; (a) an example of good SNR at all *b*-values; (b) poor SNR at *b*=1600 s/mm^2 where anatomical features of gland are barely above noise floor thus are prone to biased ADC values; (c) modest SNR in normal gland at *b*=1600 s/mm^2 although good SNR in lesion due to low ADC (yellow arrows); (d) poor SNR at *b*=1600 s/mm^2 plus a ghost artifact (blue arrows) leads to bias and artifactual ADC.

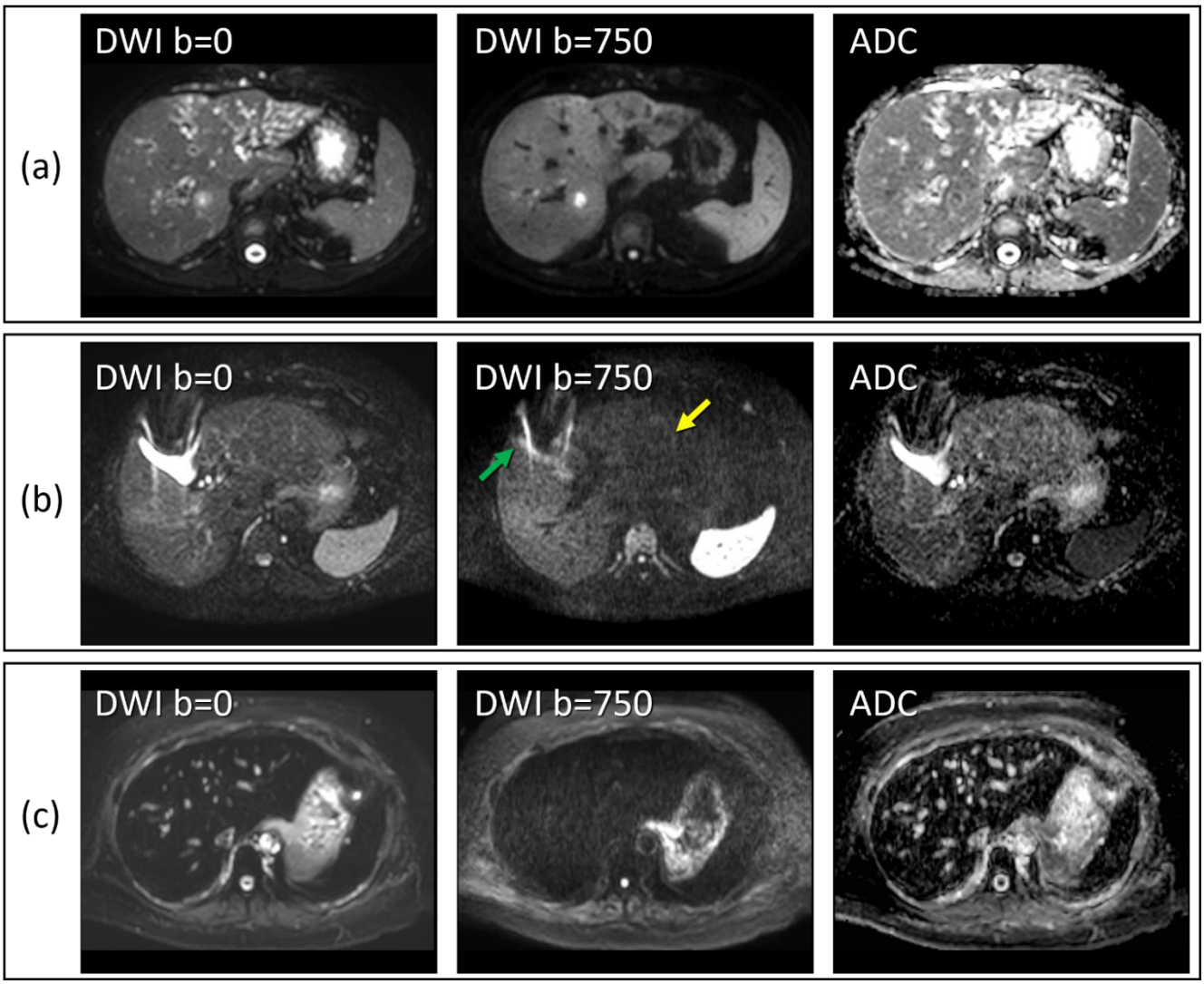

Figure 3: Visual assessment of SNR in liver DWI; (a) an example of good SNR at low and high *b*-values; (b) poor SNR particularly in left lobe at *b*=750 s/mm^2 (yellow arrow) and distortion due to metal (green arrow); and (c) poor SNR at both *b*-values where anatomical features of the liver are lost.

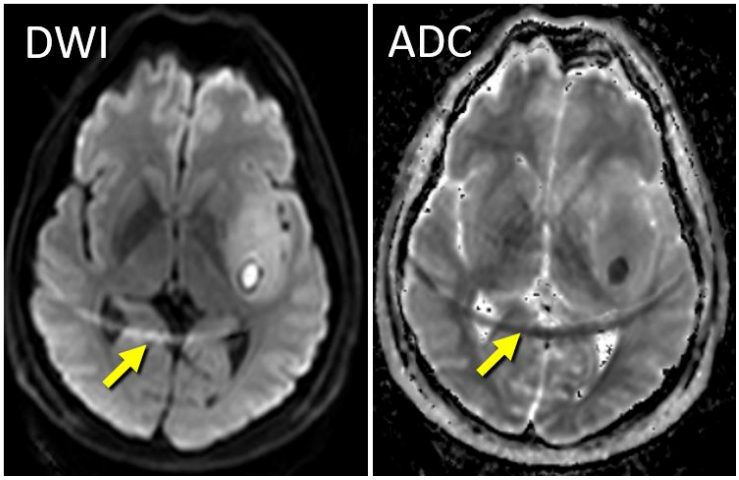

Figure 4: Ghost/parallel imaging artifact (arrows) replicates and shifts distant anatomical structures (posterior scalp in this example) along the phase-encode direction, thereby creating erroneous ADC values

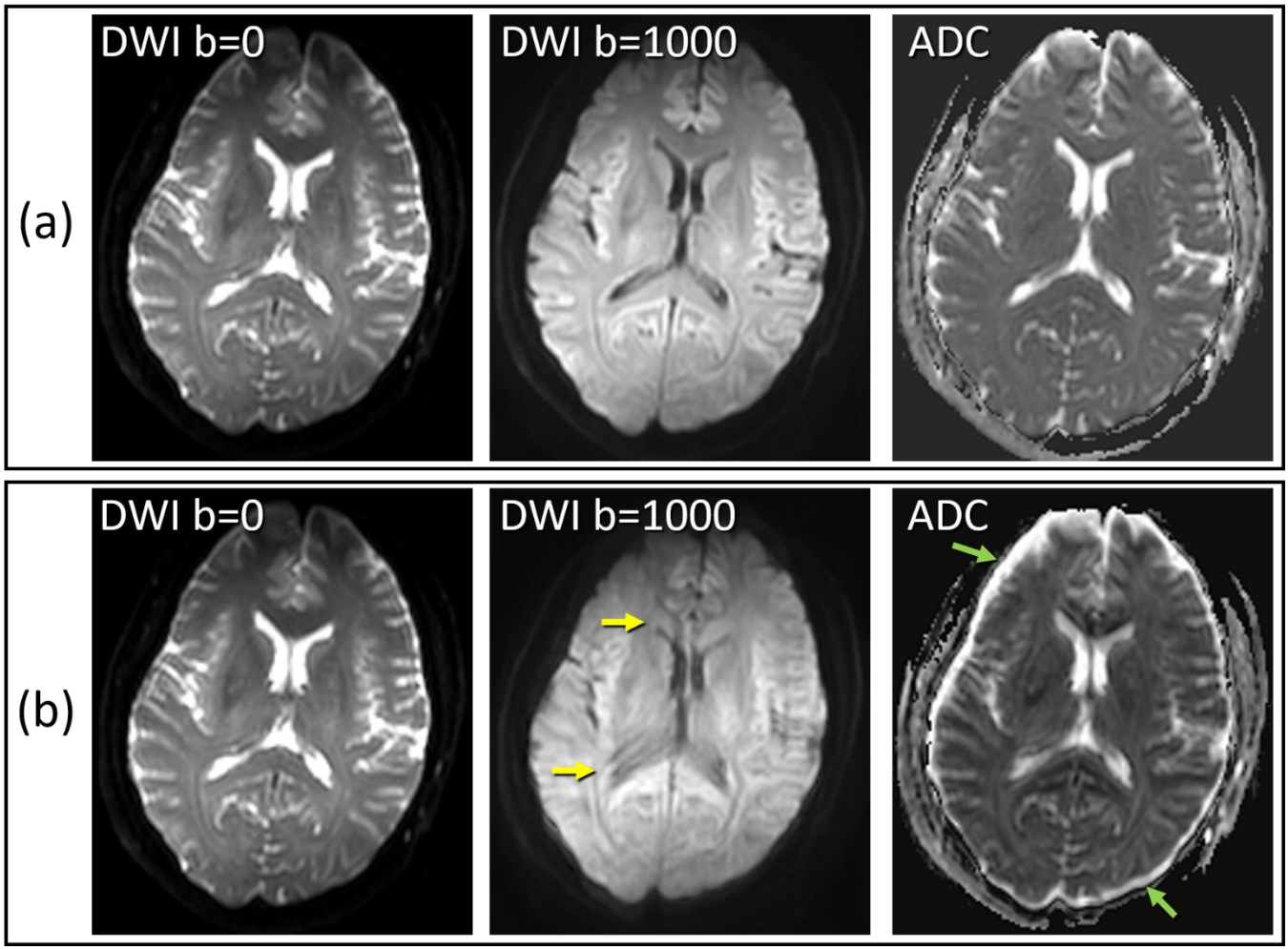

Figure 5: visual evidence of eddy currents in brain DWI. (a) Good quality DWI with no evidence of blur or spatial misalignment between low and high *b*-value DWI, thus no or low eddy current artifact. (b) Blur of anatomy on high *b*-value DWI (yellow arrows) relative to the *b*=0 DWI, plus blur and exaggerated thickness of the CSF rind around the brain (green arrows) relative to the CSF space on *b*=0 DWI are evidence of an eddy current artifact.

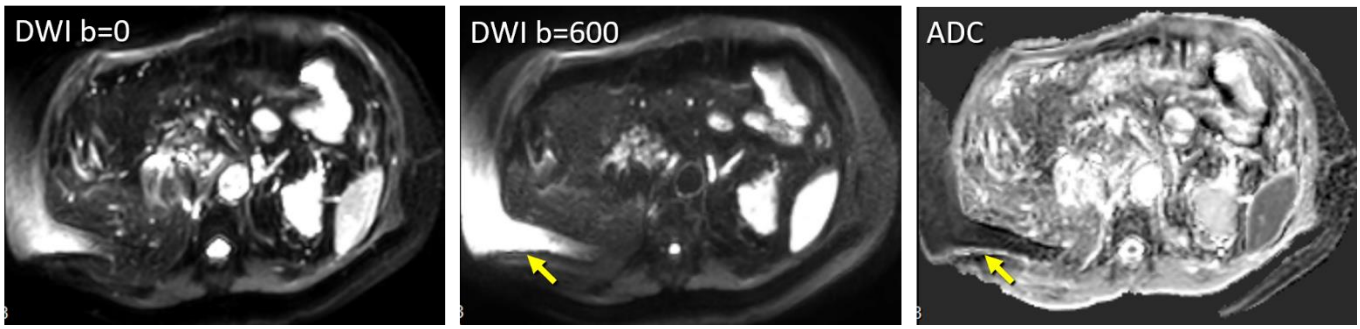

Figure 6: Unsuppressed fat signal spatially shifted on SS-EPI DWI (shifts several cm along phase-encode direction) can obscure the tissue of interest (arrow). Exceptionally low ADC of fat renders ADC meaningless in tissue superimposed by a residual fat signal.

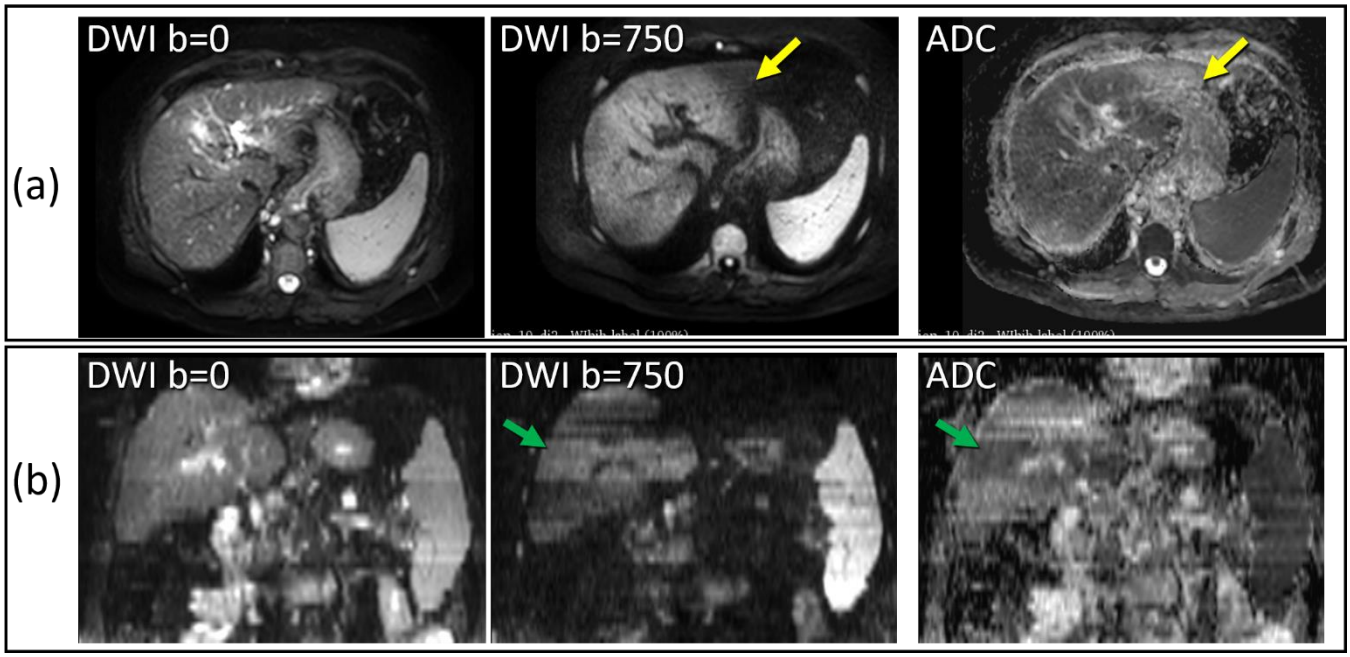

Figure 7: Visual assessment of motion artifact in liver DWI. (a) Areas of low signal on high *b*-value relative to adjacent tissue may result from motion. Cardiac pulsation transmitted to left lobe artifactually inflates ADC (yellow arrows). (b) Reformat of axial DWI/ADC to coronal can aid identification of motion artifact seen as bands on high *b*-value and ADC (green arrows).

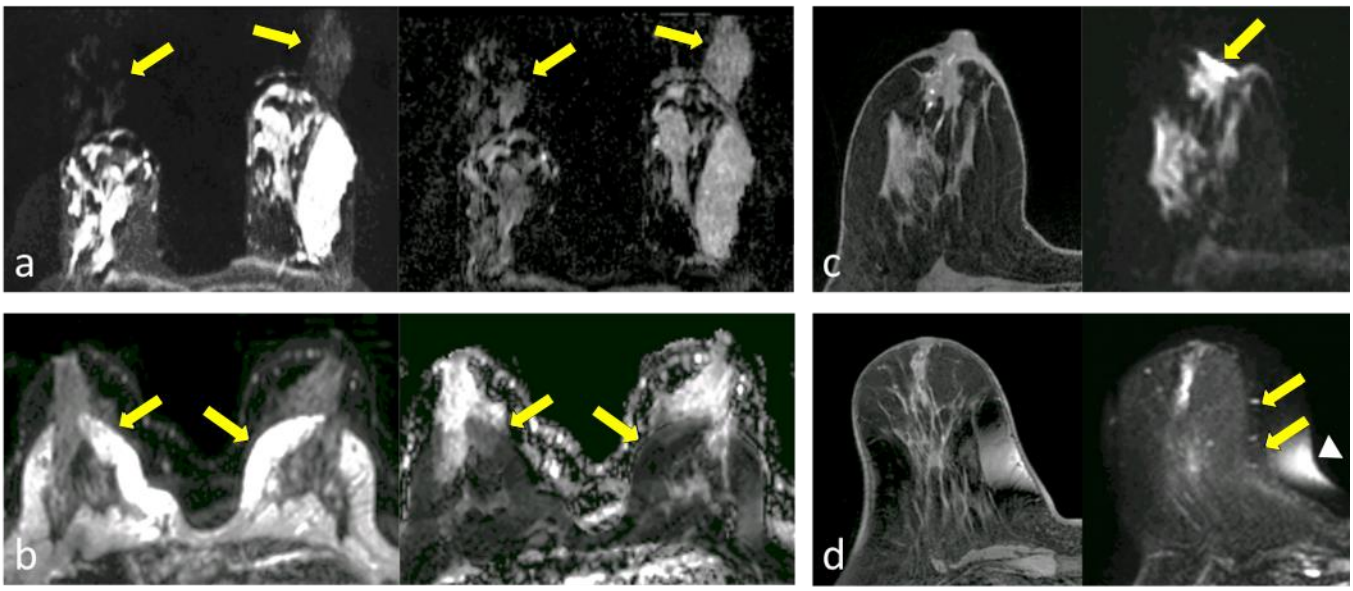

Figure 8: Common artifacts of breast DWI, illustrated in separate subjects. (a) Nyquist ghost artifact, appearing at N/4 due to parallel imaging undersampling, duplicating signal from the parenchyma on DWI (left) and resulting ADC map (right). (b) Detrimental chemical shift artifacts on DWI (left, arrows) due to poor fat suppression, causing artifactual reductions of ADC within the breast parenchyma (right, arrows). (c) Magnetic susceptibility artifact (arrow) causing distortion at air/tissue skin surface on DWI (right) compared with undistorted T1-weighted image (left). (d) Spatial distortion (arrows) and chemical shift artifact (arrowhead) of DWI due to poor shimming compared with undistorted T1-weighted image (left). (Figure adapted from Partridge et al. J. MAGN. RESON. IMAGING 2017;**45**:337–355 111)

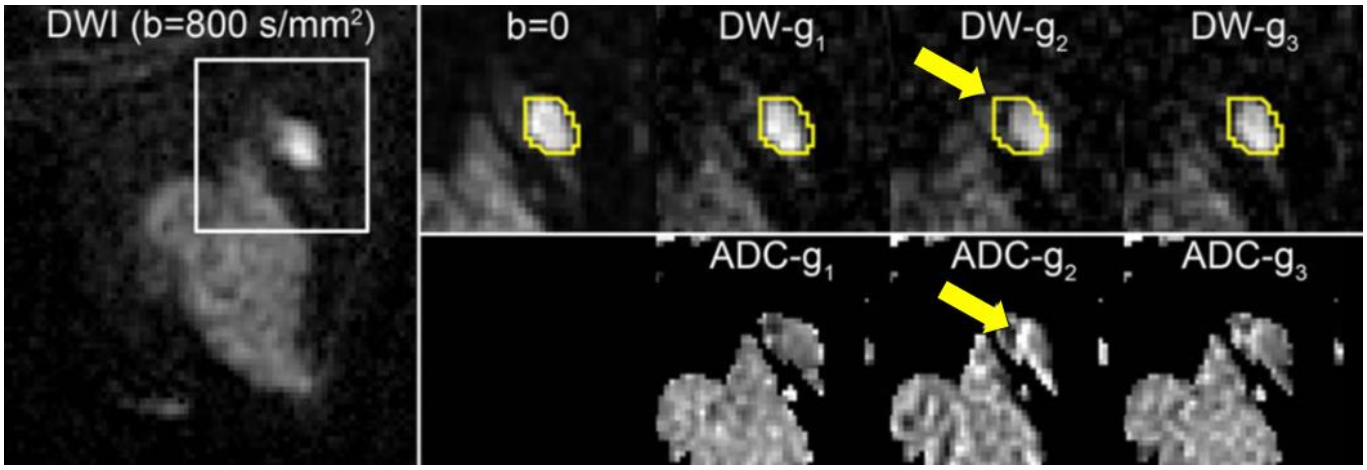

FIGURE 9: Spatial misregistration between images within a DWI sequence representing eddy-current artifact. A breast lesion is visible in the lateral breast on the averaged DW image (b=800 s/mm^2, left). White box shows region of magnification. A contour of the lesion defined on b=0 and propagated to the individual gradient direction DW images for the same slice shows the lesion is shifted (arrow) in the DW-g_2 image (obtained with diffusion gradients applied in the g_2 direction) with respect to the b=50 s/mm^2 image and other b=800 s/mm^2 images (obtained with gradients in the orthogonal g_1 and g_3 directions), owing to eddy-current effects. This misalignment causes an artifactual increase in ADC at the edge of the lesion on the corresponding ADC map (below). (Figure adapted from Partridge et al., J. Magn Reson Imaging 2017;**45**:337–355 [111])

3.12. Image Distribution

This activity describes criteria and procedures related to distributing, transferring and archiving images and metadata that are necessary to reliably meet the Profile Claim.

3.12.1 DISCUSSION

Images are distributed via network using the Digital Imaging and Communications in Medicine (DICOM) transfer protocol as per standard local practice. Along with required trace DWI DICOM, individual directional DWI and ADC maps (if generated on the scanner as DICOM images) should be archived. DWI DICOM tags that store this information currently vary among vendors. Directional DWIs may inform users about motion, eddy currents, or gradient non-linearities that are specific to a given direction, particularly when assessing scanner performance by use of a phantom with known properties. Trace DWI for each b-value should be stored in the local PACS for offline generation of ADC maps on image analysis workstations.

Absolute image scaling and units of generated ADC maps must be available and ideally stored in public DICOM tags such as RealWorldValueMapping [0040,9096], RescaleIntercept [0028,1052], RescaleSlope [0028,1053] and RescaleType [0028,1054] such that ADC map values are properly interpretable (e.g., "A true diffusion coefficient of 1.1x10^{-3} mm^2/s is represented by an ADC map pixel/ROI value on the analysis workstation as 1100."). DICOM Parametric Map object [112] should be considered for storage of ADC maps, as it provides unambiguous encoding of the quantity, units, b-values used and derivation method used for ADC calculation [113]. The use of DICOM Parametric Map can facilitate interoperable and standardized description of the DWI analysis results. It is noted that this object type is a recent introduction to the DICOM standard and is not widely adopted among the vendors [112, 113].

For image QA and protocol optimization, it is preferable to have full *b*-matrix values and diffusion encoding times provided by the vendors, so that they may be recorded in the appropriate fields in the DICOM file and reflected in the vendor DICOM conformance statement.

3.12.2 SPECIFICATION

Parameter	Actor	Requirement
ADC maps	Scanner Operator	ADC maps shall be preserved with DICOM scale tags. ADC map scale/units and *b*-values used for generation shall be recorded.
Image DICOM	Acquisition Device	DICOM tags essential for downstream review and diffusion analysis shall be maintained including pixel intensity scaling [114], *b*-value, and DWI directionality vs. trace, and ADC scale and units. Trace DWI DICOM at each *b*-value shall be archived in the local PACS.

3.13. Image Analysis

This activity describes criteria and procedures related to producing quantitative measurements from the images that are necessary to reliably meet the Profile Claim.

3.13.1 DISCUSSION

ADC maps used for offline image analysis must be equivalent to ADC maps generated on the MRI system. That is, all software elements (here referred to as "Image Analysis Tool") including the image handling/network chain must appropriately deal with potential DICOM scaling of DWI and ADC pixel values [114] and fit algorithm bias, otherwise quantitative content may be lost. The level of "equivalence" is expected to be well within the ROI standard deviation. Discrepancy comparable to or greater than the standard deviation suggests erroneous scaling of the ADC map by the image analysis software, possibly due to incorrect or missing DICOM information. Any such discrepancy must be resolved before proceeding with statistical analysis for profile compliance.

When the image analysis software is used to generate ADC maps from source DWI, the software must use a mono exponential model of DWI signal versus *b*-value. Offline image analysis software must be able to extract *b*-value and diffusion axis direction content from the DICOM header to appropriately derive ADC maps (e.g., from isotropic or trace DWI). The resulting ADC maps should also have associated scale and unit meta-data saved for quantitative analysis, i.e., in an ITK-compatible format (such as NIFTI or MHD) or as a parametric map DICOM. The numerical software conformance and signal-to-noise sensitivity (bias and range linearity with respect to ground-truth ADC values) can be tested over the range of *b*-values and tissue-like ADC using the DWI digital reference object [101], available on the QIDW (https://tinyurl.com/DWIConformanceResources). The choice of fit algorithm (log-linear vs. a non-linear exponential model) can also be informed by DWI DRO analysis to minimize noise-induced errors and biases.

For longitudinal analysis, level and range of slices with tissue/tumor of interest should be reasonably matched each time the measurements are performed. Ancillary MR images (e.g., high *b*-value DWI, T_1-weighted, T_2-weighted, post-gadolinium) that best contrast the lesion of interest, can aid ROI placement [21, 68, 69] on ADC maps. Tissue or lesion ADC quantification requires ROI delineation in two or three-dimensions. Ideally, ROI geometry is retained for future reference. The ROI is chosen by the radiologist to

match the same lesion/tissue assayed on prior time points, though the ROI size may change in longitudinal imaging of a given lesion due to treatment response or disease progression. Selected ROI size should be sufficient to represent the targeted ADC statistics. That is, ROIs should be large enough to avoid ADC values being unduly influenced by random image noise and/or under-sampled regional heterogeneity. Procedural steps to create and extract quantities from ROIs vary among software packages. At times, histogram analysis of whole tumor ROIs may be preferable to allow for distinction between predominantly solid and heterogeneous cystic/necrotic lesions depending on organ systems.

3.13.1.1 Brain

In brain, avoid contamination within the ROI from tissues such as CSF or that may have high iron content, such as acute or chronic hemorrhagic areas that have anomalous ADC values. The brain may also contain areas of large necrotic cysts and surgical cavities – these areas should be avoided.

3.13.1.2 Liver

For liver parenchyma evaluation, ROI placement should avoid large vessels or extraneous anomalous ADC tissue unrelated to target tissue of interest such as cysts or hemangiomas. Comparison of DWI at b=0 having high SNR revealing both vessels and focal lesions, to moderately low b (< 100 s/mm^2) where vessels are suppressed can be useful to localize lesions. It is also important when assessing the ADC of liver parenchyma to avoid the lateral segment of the left lobe, as this area is subject to pulsatile effects from the heart, leading to bias in high ADC values.

For large liver lesions, special consideration should be given to lesion heterogeneity. Avoidance of central necrosis or cystic degeneration is recommended so that the quantitative assay is limited to areas of solid tissue/tumor.

3.13.1.3 Prostate

Prostate ROIs should be manually placed on axial images by the radiologist where the tissues of interest are adequately conspicuous on the DWI, such as high b-value and/or ADC maps, or identifiable guided by ancillary MR images.

3.13.1.4 Breast

In breast, avoid contamination within the ROI from areas that have anomalous ADC values due to poor fat suppression, biopsy hemorrhage, necrotic cysts and surgical cavities.

3.13.2 SPECIFICATION

Parameter	Actor	Requirement
ROI Determination	Image Analyst	Shall segment the ROI on ADC maps consistently across time points using the same software / analysis package guided by a fixed set of image contrasts and avoiding artifacts
ROI geometry		Screenshot(s) documenting ROI placement on ADC maps shall be retained in the subject database for future reference ROI as a binary pixel mask in image coordinates is desired in the subject database for future reference. Ideally, ROI shall be saved as a DICOM segment object

Image Display	Image Analysis Tool	Software shall allow operator-defined ROI analysis of DWI/ADC aided by inspection of ancillary MR contrasts Ideally, above plus multi view-port display where DWI/ADC and ancillary MR contrasts from the same scan date are displayed side-by-side and geometrically linked per DICOM (e.g., cursor; crosshair; ROI; automatically replicated in all view-ports); ROIs/VOIs may include multiple noncontiguous areas on one slice and/or over multiple slices
Analysis Procedure		Analysis steps, derived metrics and analysis software package shall be held constant for all subjects and serial time points
ADC statistics		Shall allow display and retention of ROI statistics in patient DICOM database (PACS). Statistics shall include ADC mean, standard deviation, and ROI/VOI area/volume Ideally, ADC pixel histogram, additional statistics for ADC maximum, minimum, exclusion of "NaNs", and explicit recording of inclusion or exclusion of "zero-valued pixels shall be retained with the statistics
Fit algorithm type		The specific choice of the fit algorithm (e.g., linear fit to logarithmic SI vs. non-linear fit with Rician noise, a particular scanner software version, etc.) shall be recorded, held constant within a study and reported with any dissemination of study findings.
Fit algorithm bias		For offline ADC map generation, the mean ADC shall agree with scanner-generated, or DRO ground truth, ADC values to within one ROI standard deviation.
b-value and direction		Software shall extract *b*-values and diffusion axis direction from DICOM header
Phantom ADC QC metrics		Software with independent QA option shall evaluate and report phantom scan protocol compliance and ADC metrics including bias, random error, linearity, DWI SNR, *b*-value dependence, and spatial uniformity according to Table 3.2.2 to enable performance assessment for Site qualification (3.2) and periodic QA (3.5)

4. Assessment Procedures

Most of the requirements described in Section 3 can be assessed for conformance by direct observation, however some of the performance-oriented requirements are assessed using a procedure. When a specific assessment procedure is required or to provide clarity, those procedures are defined in subsections here in Section 4 and the subsection is referenced from the corresponding requirement in Section 3.

4.1. Assessment Procedure: ADC bias and precision

To satisfy site qualification specs for multi-site trial (3.2.2), the baseline ADC measurement bias and precision [30, 34-36] (Appendix E.1) for a given MRI system will be assessed near isocenter using a quantitative DWI phantom. This phantom should contain media with known diffusion properties, similar to ice water-based DWI phantoms [61, 62, 115] or the QIBA DWI phantom [64] also known as the CaliberMRI, Inc. Model 128 (see https://www.qmri.com). Details for preparation and use of the QIBA DWI phantom are available in the QIBA DWI wiki. "QibaPhanR1.4" software provided through the QIDW or CaliberMRI, Inc. qCal-MR, can be used to generate the relevant assessment metrics on a highly automated basis. The assessment procedure is described in detail in Appendix E.1, and will include the following steps:

- Preparation of temperature-controlled DWI phantom to allow sufficient time for the sample to achieve thermal equilibrium (≥ 1 hour) and maintain during scanning (~ 1 hr).
- Implementation of the system-specific scan protocol including the DWI scan parameters defined in Appendix D, Table D.1.
- Defining the "Patient Landmark" on the center of the phantom and keeping the prescription of slices centered on Superior/Inferior=0 mm (for horizontal bore magnets).
- Acquisition of DWI scans according to pre-built protocol and exporting generated trace-DWI DICOM preserving the required metadata for protocol compliance check.
- Loading DWI DICOM into the image analysis SW and checking compliance of the header metadata with the allowed scan parameter ranges.
- Calculation of corresponding ADC maps using mono-exponential signal decay model between available pairs of *b*-values, according to $ADC_{bmin,b} = \frac{1}{(b-bmin)} \ln\left[\frac{S_{bmin}}{S_b}\right]$
- Defining 1-2 cm ROI (> 80 pixels) with minimal offset from isocenter on ADC images with uniform signal, avoiding artifacts and edges.
- Estimation of mean ADC bias (BS_{ADC}) in respect to true diffusion constant (DC_{true}) of the phantom medium and confidence interval within ROI containing *N* pixels with *mean(ADC)*= μ and standard deviation *SD(ADC)*= σ: $BS_{ADC} \pm CI = (\mu - DC_{true}) \pm 1.96 \frac{\sigma}{\sqrt{N}}$
- Estimation of the random measurement error (precision) within ROI as: $\%CV = 100\% \cdot \frac{\sigma}{\mu}$
- Estimation of baseline short-term intra-scan repeatability (*RC*) and wCV of mean ADC measurement from sequential DWI phantom scans (per scan protocol) based on σ_w^2 intra-scan ADC variance, as: $RC = 2.77 \cdot \sigma_w$; $wCV = 100 \frac{\sigma_w}{\mu}$ (without repositioning)
- Estimation of long-term system repeatability and precision using above-mentioned formalism across multiple longitudinal (periodic QA) phantom scans, with consistent positioning and orientation (on different exam days)

4.2. Assessment Procedure: Voxel SNR

To ensure that relative system performance metric satisfies qualification requirements (3.2.2) and confirm that DWI SNR was adequate to measure ADC bias without incremental bias due to low SNR [93-95] (Appendix E.2) the following assessment steps [116-119] should be followed:

- Export and combine sequential DWI scans for the quantitative diffusion phantom at fixed *b*-value to calculate the temporal (i.e., over the "n" sequential scans) mean of DWI pixel images ("signal image") and temporal DWI pixel standard deviation images ("temporal noise image") for each *b*-value.
- When *n=2k (k=1..p "pairs" of image sets*), "temporal noise image" can be estimated by "DIFF image" = sumODD – sumEVEN, where sum all odd-numbered DWI dynamics called "sumODD image" and sum all even-numbered dynamics called "sumEVEN image".
- For the isocenter ROIs (1-2 cm diam, > 80 pixels), estimate signal-to-noise ratio *n*-scan (SNR_n) according to:
  $SNR_n = \frac{Spatial\ mean\ pixel\ value\ \ on\ Signal\ Image}{Spatial\ mean\ pixel\ value\ on\ Temporal\ Noise\ Image}$ or alternatively,
  $altSNR_n = \sqrt{n}\ \frac{Spatial\ mean\ pixel\ value\ on\ Signal\ Image}{Spatial\ standard\ deviation\ pixel\ value\ on\ DIFF\ Image}$
- Estimate $CI_{95\%}(SNR_n) = 1.96\ \frac{\sigma_{SNR}}{\sqrt{N}}$, using error propagation estimate for $SD(SNR_n)$ by $\sigma_{SNR} = SNR_n\sqrt{sCV^2 + nCV^2}$ with spatial coefficients of variance across *N*-pixel ROI (*N* > 50), sCV and nCV, for the "signal image" and "noise image", respectively.
- Similar $SNR \pm CI$ estimates can be obtained for the derived multi-scan ADC maps.
- When multiple sequential scans are not available, crudely (subject to Rician bias and background regularization) estimate "noise" level by SD in signal-free background ROI or within the isocenter ROI defined on uniform signal-producing area, and calculate background SNR estimate as:
  $SNR_{vs\ bkgnd} = \frac{Spatial\ mean\ pixel\ value\ on\ Signal\ Image}{Spatial\ standard\ deviation\ pixel\ value\ in\ background\ ROI}$
- Use above noise estimates for *b*-value CNR calculation, when "signal image" is defined as a difference between pair of (different) *b*-value DWIs.

4.3. Assessment Procedure: ADC *b*-value Dependence

To assess whether an MRI system exhibits artifactual *b*-value dependence in ADC measurement (Appendix E.3) and to satisfy linearity qualification requirements (3.2.2) for this Profile, the assessor will use the following procedure with quantitative diffusion phantom DWI:

- Calculate ADC maps between available pairs of *b*-values, according to $ADC_{bmin,b} = \frac{1}{(b-bmin)}\ \ln\left[\frac{S_{bmin}}{S_b}\right]$
- Compare ADC values measured for isocenter ROI for $b_2 \neq b_1$ pairs, using both $(b_1 - b_{min})$ and $(b_2 - b_{min}) \geq 400$ s/mm^2, as: $ADC\ bvalue\ dependence = 100\%\ \left\|\frac{(ADC_{bmin,b2} - ADC_{bmin,b1})}{ADC_{bmin,b1}}\right\|$

4.4. Assessment Procedure: ADC Spatial Bias

To assess spatial uniformity of diffusion weighting [62, 120] in respect to nominal *b*-value at isocenter and to meet baseline qualification specs (3.2.2, Appendix E.4) for specific study protocol:

- Select uniform quantitative DWI phantom with known, or measured at isocenter, ADC value and geometry that spans the imaging volume for the studied organ and fits in the application-specific receiver coil
- Perform DWI phantom scans including locations offset from isocenter and derive ADC maps.
- Define multiple ROIs offset from isocenter and spanning the imaged volume, and map the offset-dependence for the mean ADC values.
- Calculate ADC bias with respect to known phantom value as a function of the offset from isocenter.
- Compare the measured bias with the maximum allowed by specifications in Section 3.2.2.

4.5. Assessment Procedure: Image Analysis Software

This procedure assesses the ability of analysis SW to properly interpret quantitative header metadata (image scaling, *b*-value and directionality, Section 3.13) and the fidelity of the DWI fitting algorithm to yield unbiased ADC estimate in presence of Rician noise (e.g., Appendix E.2, Figure E.1).

- For the phantom or subject with known "reference" ADC, generate ADC maps and ROI measurements (e.g., mean and SD for ADC over a 1 cm circular ROI) on the scanner console and save the screen-capture
- Replicate the ROI placement on the images loaded to off-scanner analysis SW and confirm equivalence of displayed values and units to the on-scanner reference values.
- Load acquired reference DWI DICOM into offline analysis SW and derive ADC maps using the fit algorithm of choice. Compare offline ADC mean and SD to the on-scanner reference ROI ADC value
- Load DWI DRO DICOM (e.g., provided by QIDW) into the analysis SW and derive ADC maps using the fit algorithm of choice (e.g., non-linear exponential, or log-intensity linear fit).
- Compare derived parametric ADC maps with known DRO input to estimate bias and SD with respect to true values as a function of SNR and ADC over the ranges relevant for the specific organs.

References

1. Baehring, J.M. and R.K. Fulbright, *Diffusion-weighted MRI in neuro-oncology.* CNS Oncol, 2012. **1**(2): p. 155-67.
2. Barboriak, D.P., *Imaging of brain tumors with diffusion-weighted and diffusion tensor MR imaging.* Magn Reson Imaging Clin N Am, 2003. **11**(3): p. 379-401.
3. Chenevert, T.L., et al., *Diffusion MRI: a new strategy for assessment of cancer therapeutic efficacy.* Mol Imaging, 2002. **1**(4): p. 336-43.
4. deSouza, N.M., A. Rockall, and S. Freeman, *Functional MR Imaging in Gynecologic Cancer.* Magn Reson Imaging Clin N Am, 2016. **24**(1): p. 205-22.
5. Galban, S., et al., *Diffusion-weighted MRI for assessment of early cancer treatment response.* Curr Pharm Biotechnol, 2010. **11**(6): p. 701-8.
6. Gao, X., et al., *Magnetic resonance imaging in assessment of treatment response of gamma knife for brain tumors.* Chin Med J (Engl), 2011. **124**(12): p. 1906-10.
7. Garcia-Figueiras, R., A.R. Padhani, and S. Baleato-Gonzalez, *Therapy Monitoring with Functional and Molecular MR Imaging.* Magn Reson Imaging Clin N Am, 2016. **24**(1): p. 261-88.
8. Higano, S., et al., *Malignant astrocytic tumors: clinical importance of apparent diffusion coefficient in prediction of grade and prognosis.* Radiology, 2006. **241**(3): p. 839-46.
9. Kang, Y., et al., *Gliomas: Histogram analysis of apparent diffusion coefficient maps with standard- or high-b-value diffusion-weighted MR imaging--correlation with tumor grade.* Radiology, 2011. **261**(3): p. 882-90.
10. Kim, M. and H.S. Kim, *Emerging Techniques in Brain Tumor Imaging: What Radiologists Need to Know.* Korean J Radiol, 2016. **17**(5): p. 598-619.
11. Kim, S., et al., *Diffusion-weighted magnetic resonance imaging for predicting and detecting early response to chemoradiation therapy of squamous cell carcinomas of the head and neck.* Clin Cancer Res, 2009. **15**(3): p. 986-94.
12. Koh, D.M., et al., *Body Diffusion-weighted MR Imaging in Oncology: Imaging at 3 T.* Magn Reson Imaging Clin N Am, 2016. **24**(1): p. 31-44.
13. Lupo, J.M. and S.J. Nelson, *Advanced magnetic resonance imaging methods for planning and monitoring radiation therapy in patients with high-grade glioma.* Semin Radiat Oncol, 2014. **24**(4): p. 248-58.
14. Maier, S.E., Y. Sun, and R.V. Mulkern, *Diffusion imaging of brain tumors.* NMR Biomed, 2010. **23**(7): p. 849-64.
15. Murakami, R., et al., *Grading astrocytic tumors by using apparent diffusion coefficient parameters: superiority of a one- versus two-parameter pilot method.* Radiology, 2009. **251**(3): p. 838-45.
16. Nelson, S.J., *Assessment of therapeutic response and treatment planning for brain tumors using metabolic and physiological MRI.* NMR Biomed, 2011. **24**(6): p. 734-49.
17. Padhani, A.R., *Diffusion magnetic resonance imaging in cancer patient management.* Semin Radiat Oncol, 2011. **21**(2): p. 119-40.
18. Padhani, A.R. and A. Gogbashian, *Bony metastases: assessing response to therapy with whole-body diffusion MRI.* Cancer Imaging, 2011. **11 Spec No A**: p. S129-45.
19. Padhani, A.R. and D.M. Koh, *Diffusion MR imaging for monitoring of treatment response.* Magn Reson Imaging Clin N Am, 2011. **19**(1): p. 181-209.
20. Padhani, A.R., D.M. Koh, and D.J. Collins, *Whole-body diffusion-weighted MR imaging in cancer: current status and research directions.* Radiology, 2011. **261**(3): p. 700-18.
21. Padhani, A.R., et al., *Diffusion-weighted magnetic resonance imaging as a cancer biomarker: consensus and recommendations.* Neoplasia, 2009. **11**(2): p. 102-25.
22. Patterson, D.M., A.R. Padhani, and D.J. Collins, *Technology insight: water diffusion MRI--a potential new biomarker of response to cancer therapy.* Nat Clin Pract Oncol, 2008. **5**(4): p. 220-33.
23. Pope, W.B., et al., *Recurrent glioblastoma multiforme: ADC histogram analysis predicts response to bevacizumab treatment.* Radiology, 2009. **252**(1): p. 182-9.
24. Provenzale, J.M., S. Mukundan, and D.P. Barboriak, *Diffusion-weighted and perfusion MR imaging for brain tumor characterization and assessment of treatment response.* Radiology, 2006. **239**(3): p. 632-49.
25. Rosenkrantz, A.B., et al., *Body diffusion kurtosis imaging: Basic principles, applications, and considerations for clinical practice.* J Magn Reson Imaging, 2015. **42**(5): p. 1190-202.

26. Schmainda, K.M., *Diffusion-weighted MRI as a biomarker for treatment response in glioma.* CNS Oncol, 2012. **1**(2): p. 169-80.
27. Shiroishi, M.S., J.L. Boxerman, and W.B. Pope, *Physiologic MRI for assessment of response to therapy and prognosis in glioblastoma.* Neuro Oncol, 2016. **18**(4): p. 467-78.
28. Taouli, B. and D.M. Koh, *Diffusion-weighted MR imaging of the liver.* Radiology, 2010. **254**(1): p. 47-66.
29. Yamasaki, F., et al., *Apparent diffusion coefficient of human brain tumors at MR imaging.* Radiology, 2005. **235**(3): p. 985-91.
30. Barnhart, H.X. and D.P. Barboriak, *Applications of the repeatability of quantitative imaging biomarkers: a review of statistical analysis of repeat data sets.* Transl Oncol, 2009. **2**(4): p. 231-5.
31. Goldmacher, G.V., et al., *Standardized Brain Tumor Imaging Protocol for Clinical Trials.* AJNR Am J Neuroradiol, 2015. **36**(10): p. E65-6.
32. Jackson, E.F., et al., *Magnetic resonance assessment of response to therapy: tumor change measurement, truth data and error sources.* Transl Oncol, 2009. **2**(4): p. 211-5.
33. Meyer, C.R., et al., *Quantitative imaging to assess tumor response to therapy: common themes of measurement, truth data, and error sources.* Transl Oncol, 2009. **2**(4): p. 198-210.
34. Obuchowski, N.A., et al., *Statistical Issues in Testing Conformance with the Quantitative Imaging Biomarker Alliance (QIBA) Profile Claims.* Acad Radiol, 2016. **23**(4): p. 496-506.
35. Obuchowski, N.A., et al., *Quantitative imaging biomarkers: a review of statistical methods for computer algorithm comparisons.* Stat Methods Med Res, 2015. **24**(1): p. 68-106.
36. Raunig, D.L., et al., *Quantitative imaging biomarkers: a review of statistical methods for technical performance assessment.* Stat Methods Med Res, 2015. **24**(1): p. 27-67.
37. Sullivan, D.C., et al., *Metrology Standards for Quantitative Imaging Biomarkers.* Radiology, 2015. **277**(3): p. 813-25.
38. Li, S.P. and A.R. Padhani, *Tumor response assessments with diffusion and perfusion MRI.* J Magn Reson Imaging, 2012. **35**(4): p. 745-63.
39. O'Connor, J.P., et al., *Imaging biomarker roadmap for cancer studies.* Nat Rev Clin Oncol, 2016.
40. Partridge, S.C., et al., *Diffusion-weighted MRI Findings Predict Pathologic Response in Neoadjuvant Treatment of Breast Cancer: The ACRIN 6698 Multicenter Trial.* Radiology, 2018. **289**(3): p. 618-627.
41. Chenevert, T.L., P.C. Sundgren, and B.D. Ross, *Diffusion imaging: insight to cell status and cytoarchitecture.* Neuroimaging Clin N Am, 2006. **16**(4): p. 619-32, viii-ix.
42. Ross, B.D., et al., *Evaluation of cancer therapy using diffusion magnetic resonance imaging.* Mol Cancer Ther, 2003. **2**(6): p. 581-7.
43. Li, W., et al., *Diffusion-Weighted MRI for Predicting Pathologic Complete Response in Neoadjuvant Immunotherapy.* Cancers (Basel), 2022. **14**(18).
44. Newitt, D.C., et al., *Test-retest repeatability and reproducibility of ADC measures by breast DWI: Results from the ACRIN 6698 trial.* J Magn Reson Imaging, 2018.
45. Sorace, A.G., et al., *Repeatability, reproducibility, and accuracy of quantitative mri of the breast in the community radiology setting.* J Magn Reson Imaging, 2018.
46. Bonekamp, D., et al., *Diffusion tensor imaging in children and adolescents: reproducibility, hemispheric, and age-related differences.* Neuroimage, 2007. **34**(2): p. 733-42.
47. Paldino, M.J., et al., *Repeatability of quantitative parameters derived from diffusion tensor imaging in patients with glioblastoma multiforme.* J Magn Reson Imaging, 2009. **29**(5): p. 1199-205.
48. Pfefferbaum, A., E. Adalsteinsson, and E.V. Sullivan, *Replicability of diffusion tensor imaging measurements of fractional anisotropy and trace in brain.* J Magn Reson Imaging, 2003. **18**(4): p. 427-33.
49. Braithwaite, A.C., et al., *Short- and midterm reproducibility of apparent diffusion coefficient measurements at 3.0-T diffusion-weighted imaging of the abdomen.* Radiology, 2009. **250**(2): p. 459-65.
50. Deckers, F., et al., *Apparent diffusion coefficient measurements as very early predictive markers of response to chemotherapy in hepatic metastasis: a preliminary investigation of reproducibility and diagnostic value.* J Magn Reson Imaging, 2014. **40**(2): p. 448-56.
51. Heijmen, L., et al., *Diffusion-weighted MR imaging in liver metastases of colorectal cancer: reproducibility and biological validation.* Eur Radiol, 2013. **23**(3): p. 748-56.
52. Miquel, M.E., et al., *In vitro and in vivo repeatability of abdominal diffusion-weighted MRI.* Br J Radiol, 2012. **85**(1019): p. 1507-12.
53. Gibbs, P., Pickles, M.D., L.W. Turnbull, *Repeatability of echo-planar-based diffusion measurements of the*

human prostate at 3T. Magn Reson Imaging, 2007. **25**(10): p. 1423-9.
54. Jambor, I., et al., *Optimization of b-value distribution for biexponential diffusion-weighted MR imaging of normal prostate.* J Magn Reson Imaging, 2014. **39**(5): p. 1213-22.
55. Jambor, I., et al., *Evaluation of different mathematical models for diffusion-weighted imaging of normal prostate and prostate cancer using high b-values: a repeatability study.* Magn Reson Med, 2015. **73**(5): p. 1988-98.
56. Litjens, G.J., et al., *Interpatient variation in normal peripheral zone apparent diffusion coefficient: effect on the prediction of prostate cancer aggressiveness.* Radiology, 2012. **265**(1): p. 260-6.
57. Fedorov, A., et al., *Multiparametric MRI of the prostate: repeatability of volume and apparent diffusion coefficient quantification.* Invest Radiol, 2017. **52**: p. 538-46.
58. Afaq, A., et al., *Clinical utility of diffusion-weighted magnetic resonance imaging in prostate cancer.* BJU Int, 2011. **108**(11): p. 1716-22.
59. Winfield, J.M., et al., *Extracranial Soft-Tissue Tumors: Repeatability of Apparent Diffusion Coefficient Estimates from Diffusion-weighted MR Imaging.* Radiology, 2017: p. 161965.
60. Hegde, J.V., et al., *Multiparametric MRI of prostate cancer: an update on state-of-the-art techniques and their performance in detecting and localizing prostate cancer.* J Magn Reson Imaging, 2013. **37**(5): p. 1035-54.
61. Chenevert, T.L., et al., *Diffusion coefficient measurement using a temperature-controlled fluid for quality control in multicenter studies.* J Magn Reson Imaging, 2011. **34**(4): p. 983-7.
62. Malyarenko, D.I., et al., *Demonstration of nonlinearity bias in the measurement of the apparent diffusion coefficient in multicenter trials.* Magn Reson Med, 2016. **75**(3): p. 1312-23.
63. Pierpaoli, C., et al. *Polyvinylpyrrolidone (PVP) water solutions as isotropic phantoms for diffusion MRI studies.* in *ISMRM 17th annual meeting*. 2009. Honolulu, HI.
64. Boss, M.A., et al. *Temperature-Controlled Isotropic Diffusion Phantom with Wide Range of Apparent Diffusion Coefficients for Multicenter Assessment of Scanner Repeatability and Reproducibility*. in *Proceeding of the International Society of Magnetic Resonance in Medicine*. 2014. Milan, Italy.
65. Malyarenko, D., et al., *Multi-system repeatability and reproducibility of apparent diffusion coefficient measurement using an ice-water phantom.* J Magn Reson Imaging, 2013. **37**(5): p. 1238-46.
66. Mulkern, R.V., et al., *Pediatric brain tumor consortium multisite assessment of apparent diffusion coefficient z-axis variation assessed with an ice-water phantom.* Acad Radiol, 2015. **22**(3): p. 363-9.
67. Palacios, E.M., et al., *Toward Precision and Reproducibility of Diffusion Tensor Imaging: A Multicenter Diffusion Phantom and Traveling Volunteer Study.* AJNR Am J Neuroradiol, 2017. **38**(3): p. 537-545.
68. Ellingson, B.M., et al., *Diffusion MRI quality control and functional diffusion map results in ACRIN 6677/RTOG 0625: a multicenter, randomized, phase II trial of bevacizumab and chemotherapy in recurrent glioblastoma.* Int J Oncol, 2015. **46**(5): p. 1883-92.
69. Ellingson, B.M., et al., *Consensus recommendations for a standardized Brain Tumor Imaging Protocol in clinical trials.* Neuro Oncol, 2015. **17**(9): p. 1188-98.
70. Barth, M., et al., *Simultaneous multislice (SMS) imaging techniques.* Magn Reson Med, 2016. **75**(1): p. 63-81.
71. Eichner, C., et al., *Slice accelerated diffusion-weighted imaging at ultra-high field strength.* Magn Reson Med, 2014. **71**(4): p. 1518-25.
72. Obele, C.C., et al., *Simultaneous Multislice Accelerated Free-Breathing Diffusion-Weighted Imaging of the Liver at 3T.* Abdom Imaging, 2015. **40**(7): p. 2323-30.
73. Wu, X., et al., *Simultaneous multislice multiband parallel radiofrequency excitation with independent slice-specific transmit B1 homogenization.* Magn Reson Med, 2013. **70**(3): p. 630-8.
74. Hamilton, J., D. Franson, and N. Seiberlich, *Recent advances in parallel imaging for MRI.* Prog Nucl Magn Reson Spectrosc, 2017. **101**: p. 71-95.
75. Barth, B.K., et al., *Diffusion-Weighted Imaging of the Prostate: Image Quality and Geometric Distortion of Readout-Segmented Versus Selective-Excitation Accelerated Acquisitions.* Invest Radiol, 2015. **50**(11): p. 785-91.
76. Chen, N.K., et al., *A robust multi-shot scan strategy for high-resolution diffusion weighted MRI enabled by multiplexed sensitivity-encoding (MUSE).* Neuroimage, 2013. **72**: p. 41-7.
77. Setsompop, K., et al., *Improving diffusion MRI using simultaneous multi-slice echo planar imaging.* Neuroimage, 2012. **63**(1): p. 569-80.
78. Singer, L., et al., *High-resolution diffusion-weighted magnetic resonance imaging in patients with locally advanced breast cancer.* Acad Radiol, 2012. **19**(5): p. 526-34.
79. Wilmes, L.J., et al., *High-resolution diffusion-weighted imaging for monitoring breast cancer treatment*

response. Acad Radiol, 2013. **20**(5): p. 581-9.
80. Deng, J., et al., *Multishot diffusion-weighted PROPELLER magnetic resonance imaging of the abdomen.* Invest Radiol, 2006. **41**(10): p. 769-75.
81. Sorensen, A.G., et al., *Hyperacute stroke: evaluation with combined multisection diffusion-weighted and hemodynamically weighted echo-planar MR imaging.* Radiology, 1996. **199**(2): p. 391-401.
82. van Gelderen, P., et al., *Water diffusion and acute stroke.* Magn Reson Med, 1994. **31**(2): p. 154-63.
83. Bastin, M.E., *Correction of eddy current-induced artefacts in diffusion tensor imaging using iterative cross-correlation.* Magn Reson Imaging, 1999. **17**(7): p. 1011-24.
84. Le Bihan, D., et al., *Artifacts and pitfalls in diffusion MRI.* J Magn Reson Imaging, 2006. **24**(3): p. 478-88.
85. Mohammadi, S., et al., *Correcting eddy current and motion effects by affine whole-brain registrations: evaluation of three-dimensional distortions and comparison with slicewise correction.* Magn Reson Med, 2010. **64**(4): p. 1047-56.
86. Dyvorne, H.A., et al., *Diffusion-weighted imaging of the liver with multiple b values: effect of diffusion gradient polarity and breathing acquisition on image quality and intravoxel incoherent motion parameters--a pilot study.* Radiology, 2013. **266**(3): p. 920-9.
87. Kakite, S., et al., *Hepatocellular carcinoma: short-term reproducibility of apparent diffusion coefficient and intravoxel incoherent motion parameters at 3.0T.* J Magn Reson Imaging, 2015. **41**(1): p. 149-56.
88. LeBihan, D., *IVIM method measures diffusion and perfusion.* Diagn Imaging (San Franc), 1990. **12**(6): p. 133, 136.
89. Lee, Y., et al., *Intravoxel incoherent motion diffusion-weighted MR imaging of the liver: effect of triggering methods on regional variability and measurement repeatability of quantitative parameters.* Radiology, 2015. **274**(2): p. 405-15.
90. Takahara, T. and T.C. Kwee, *Low b-value diffusion-weighted imaging: emerging applications in the body.* J Magn Reson Imaging, 2012. **35**(6): p. 1266-73.
91. Yoon, J.H., et al., *Evaluation of hepatic fibrosis using intravoxel incoherent motion in diffusion-weighted liver MRI.* J Comput Assist Tomogr, 2014. **38**(1): p. 110-6.
92. Merisaari, H., et al., *Fitting methods for intravoxel incoherent motion imaging of prostate cancer on region of interest level: Repeatability and gleason score prediction.* Magn Reson Med, 2017. **77**(3): p. 1249-1264.
93. Basu, S., T. Fletcher, and R. Whitaker, *Rician noise removal in diffusion tensor MRI.* Med Image Comput Comput Assist Interv, 2006. **9**(Pt 1): p. 117-25.
94. Kristoffersen, A., *Optimal estimation of the diffusion coefficient from non-averaged and averaged noisy magnitude data.* J Magn Reson, 2007. **187**(2): p. 293-305.
95. Lui, D., et al., *Monte Carlo bias field correction in endorectal diffusion imaging.* IEEE Trans Biomed Eng, 2014. **61**(2): p. 368-80.
96. Chen, N.K. and A.M. Wyrwicz, *Removal of EPI Nyquist ghost artifacts with two-dimensional phase correction.* Magn Reson Med, 2004. **51**(6): p. 1247-53.
97. Guglielmo, F.F., et al., *Hepatic MR imaging techniques, optimization, and artifacts.* Magn Reson Imaging Clin N Am, 2014. **22**(3): p. 263-82.
98. Koh, D.M., et al., *Whole-body diffusion-weighted MRI: tips, tricks, and pitfalls.* AJR Am J Roentgenol, 2012. **199**(2): p. 252-62.
99. Kuhl, C.K., et al., *Sensitivity encoding for diffusion-weighted MR imaging at 3.0 T: intraindividual comparative study.* Radiology, 2005. **234**(2): p. 517-26.
100. Grieve, S.M., A.M. Blamire, and P. Styles, *Elimination of Nyquist ghosting caused by read-out to phase-encode gradient cross-terms in EPI.* Magn Reson Med, 2002. **47**(2): p. 337-43.
101. Jackson, E.F., et al. *Acceptance Testing and Quality Assurance Procedures for Magnetic Resonance Imaging Facilities, Report of MR Subcommittee Task Group I.* 2010; Available from: http://www.aapm.org/pubs/reports/RPT_100.pdf.
102. Reese, T.G., et al., *Reduction of eddy-current-induced distortion in diffusion MRI using a twice-refocused spin echo.* Magn Reson Med, 2003. **49**(1): p. 177-82.
103. Bendel, P. and Y. Schiffenbauer, *A method for fat suppression in MRI based on diffusion-weighted imaging.* Phys Med Biol, 2010. **55**(22): p. N547-55.
104. Hansmann, J., D. Hernando, and S.B. Reeder, *Fat confounds the observed apparent diffusion coefficient in patients with hepatic steatosis.* Magn Reson Med, 2013. **69**(2): p. 545-52.
105. Hernando, D., et al., *Removal of olefinic fat chemical shift artifact in diffusion MRI.* Magn Reson Med, 2011.

65(3): p. 692-701.
106. Nagy, Z. and N. Weiskopf, *Efficient fat suppression by slice-selection gradient reversal in twice-refocused diffusion encoding.* Magn Reson Med, 2008. **60**(5): p. 1256-60.
107. Sarlls, J.E., et al., *Robust fat suppression at 3T in high-resolution diffusion-weighted single-shot echo-planar imaging of human brain.* Magn Reson Med, 2011. **66**(6): p. 1658-65.
108. Kwee, T.C., et al., *Diffusion-weighted whole-body imaging with background body signal suppression (DWIBS): features and potential applications in oncology.* Eur Radiol, 2008. **18**(9): p. 1937-52.
109. Takahara, T., et al., *Diffusion-weighted magnetic resonance imaging of the liver using tracking only navigator echo: feasibility study.* Invest Radiol, 2010. **45**(2): p. 57-63.
110. McRobbie, D.S., Scott, *Quality Control and Artefacts in Magnetic Resonance Imaging*. 2017: Institute of Physics and Engineering in Medicine. 236.
111. Partridge, S.C., et al., *Diffusion-weighted breast MRI: Clinical applications and emerging techniques.* J Magn Reson Imaging, 2017. **45**(2): p. 337-355.
112. DICOM. *Parametric Map IOD Description*. Available from: http://dicom.nema.org/medical/dicom/current/output/chtml/part03/sect_A.75.html.
113. NEMA. *ADCmodelparameters*. Available from: ftp://medical.nema.org/medical/dicom/cp/cp1665_vp_ADCmodelparameters.pdf.
114. Chenevert, T.L., et al., *Errors in Quantitative Image Analysis due to Platform-Dependent Image Scaling.* Transl Oncol, 2014. **7**(1): p. 65-71.
115. Jerome, N.P., et al., *Development of a temperature-controlled phantom for magnetic resonance quality assurance of diffusion, dynamic, and relaxometry measurements.* Med Phys, 2016. **43**(6): p. 2998.
116. Aja-Fernandez, S., C. Alberola-Lopez, and C.F. Westin, *Noise and signal estimation in magnitude MRI and Rician distributed images: a LMMSE approach.* IEEE Trans Image Process, 2008. **17**(8): p. 1383-98.
117. Sijbers, J. and A.J. den Dekker, *Maximum likelihood estimation of signal amplitude and noise variance from MR data.* Magn Reson Med, 2004. **51**(3): p. 586-94.
118. Friedman, L. and G.H. Glover, *Report on a multicenter fMRI quality assurance protocol.* J Magn Reson Imaging, 2006. **23**(6): p. 827-39.
119. Dietrich, O., et al., *Measurement of signal-to-noise ratios in MR images: influence of multichannel coils, parallel imaging, and reconstruction filters.* J Magn Reson Imaging, 2007. **26**(2): p. 375-85.
120. Bammer, R., et al., *Analysis and generalized correction of the effect of spatial gradient field distortions in diffusion-weighted imaging.* Magn Reson Med, 2003. **50**(3): p. 560-9.
121. Malkyarenko, D.I. and T.L. Chenevert, *Practical estimate of gradient nonlinearity for implementation of apparent diffusion coefficient bias correction.* J Magn Reson Imaging, 2014. **40**(6): p. 1487-95.
122. Malyarenko, D.I., et al., *Correction of Gradient Nonlinearity Bias in Quantitative Diffusion Parameters of Renal Tissue with Intra Voxel Incoherent Motion.* Tomography, 2015. **1**(2): p. 145-151.
123. Malyarenko, D.I., B.D. Ross, and T.L. Chenevert, *Analysis and correction of gradient nonlinearity bias in apparent diffusion coefficient measurements.* Magn Reson Med, 2014. **71**(3): p. 1312-23.
124. Newitt, D.C., et al., *Gradient nonlinearity correction to improve apparent diffusion coefficient accuracy and standardization in the american college of radiology imaging network 6698 breast cancer trial.* J Magn Reson Imaging, 2015. **42**(4): p. 908-19.

Appendices

Appendix A: Acknowledgements and Attributions

This document is proffered by the Radiological Society of North America [37], Diffusion-Weighted Imaging Task Force subgroup of the Perfusion Diffusion and Flow (PDF) Biomarker Committee. The PDF is composed of scientists, engineers, and clinicians representing academia, the imaging device manufacturers, image analysis software developers, image analysis laboratories, biopharmaceutical industry, government research organizations, professional societies, and regulatory agencies, among others. All work is classified as pre-competitive.

The following individuals have made critical contributions in the development of this Profile:

Edson Amaro	Nandita de Souza	Mikko Määtta	Mark Rosen
Trevor Andrews	Andrey Fedorov	Dariya Malyarenko	Samir Sharma
Rajpaul Attariwala	Clifton Fuller	Daniel Margolis	Mark Shiroishi
Daniel Barboriak	Alexander Guimaraes	Kevin Miller	Rohit Sood
David Bennett	Nola Hylton	Elizabeth Mirowski	Daniel Sullivan
Ishtiaq Bercha	Marko Ivancevic	Bastien Moreau	Ying Tang
Michael Boss	Edward Jackson	Felipe Nascimento	Bachir Taouli
Orest Boyko	Ivan Jambor	David Newitt	Aradhana Venkatesan
Martin Büchert	John Kirsch	James O'Callaghan	Lisa Wilmes
Madeline Carr	Daniel Krainak	Nancy Obuchowski	Jessica Winfield
Thomas Chenevert	Hendrik Laue	Estanislao Oubel	Ona Wu
Caroline Chung	Jiachao Liang	Savannah Partridge	Junqian Xu
Amita Shukla Dave	Chen Lin	Thorsten Persigehl	Gudrun Zahlmann

We also acknowledge the extraordinary efforts by RSNA QIBA staff in making this Profile possible.

Appendix B: Background Information

QIBA Wiki:
http://qibawiki.rsna.org/index.php/Main_Page
QIBA Perfusion, Diffusion, and Flow Biomarker Committee Wiki:
http://qibawiki.rsna.org/index.php/Perfusion,_Diffusion_and_Flow-MRI_Biomarker_Ctte
DWI Literature Review:
http://qibawiki.rsna.org/index.php/DWI_Literature_Review
QIBAPhan Analysis Software (for ADC and summary statistics of isotropic diffusion phantom):
https://tinyurl.com/DWIConformanceResources
QIBA DWI Digital Reference Object:
https://tinyurl.com/DWIConformanceResources
Diffusion Phantom Preparation and Positioning:
http://qibawiki.rsna.org/index.php/Perfusion,_Diffusion_and_Flow-MRI_Biomarker_Ctte
DICOM MR Diffusion Macro:
http://dicom.nema.org/medical/dicom/current/output/chtml/part03/sect_C.8.13.5.9.html

Appendix C: Conventions and Definitions

Apparent Diffusion Coefficient (ADC): A quantitative imaging biomarker (typically in units of mm^2/s or $\mu m^2/ms$) indicative of the mobility of water molecules. High ADC indicates free or less hindered mobility of water; low ADC indicates slow, restricted, or hindered mobility of water molecules.

***b*-value:** An indication of the strength of diffusion-weighting (typically in units of s/mm^2). It depends on a combination of gradient pulse duration, shape, strength, and the timing between diffusion gradient pulses.

DICOM: Digital Imaging and Communications in Medicine standard for distributing and viewing any kind of medical image regardless of the origin. A DWI DICOM header typically contains meta-data reflecting scan geometry and key acquisition parameters (e.g., *b*-value and gradient direction) required for subsequent generation of ADC maps and ROI statistics. A DWI DICOM macro assigns the required diffusion-specific attributes to public DICOM tags (e.g., [0018, 9087], diffusion *b*-value and [0018, 9075], diffusion directionality) which should be available independent of Vendor and scanner software version. Currently, vendors do not universally follow the DWI macro standard, storing *b*-value and direction metadata in private tags.

Diffusion Weighted Image (DWI): A type of MR image where tissue contrast is dependent on water mobility, diffusion gradient direction, concentration of water signal, and T_2 relaxation. On heavily diffusion-weighted images (i.e. high *b*-value), high signal indicates low water mobility, high proton concentration, and/or long T_2.

Isotropic (or trace) DWI: Directionally-independent diffusion-weighted images obtained as the composite (geometric average) of three orthogonal DWIs and used for ADC map derivation. Throughout this profile and assessment procedure, the term "DWI" refers to these directionally-independent images unless otherwise noted as a specific single-axis or directional DWI. Even in anisotropic media, directionally-independent (i.e. scalar) diffusion metrics are measurable using DWI combined from three-orthogonal diffusion gradient acquisitions.

Linearity: A requirement of a linear relationship between the measured ADC value and the true value over a physiologically-relevant range; the slope of this line should be equal to 1.

Ideally, to establish linearity with slope equal to 1, five truth values will be assessed, each with five repetitions. The slope may then be assessed by the following procedure:

> For each case, calculate the *ADC* (denoted Y_i), where *i* denotes the i^{th} case. Let X_i denote the true value for the i^{th} case. Fit an ordinary least squares (OLS) regression of the Y_i's on X_i's. A linear model should be fit: $Y = \beta_o + \beta_1 X$, and R^2 estimated. Let $\widehat{\beta_1}$ denote the estimated slope. Calculate its variance as $\widehat{Var}_{\beta_1} = \{\sum_{i=1}^{N}(Y_i - \hat{Y}_i)^2 / (N-2)\} / \sum_{i=1}^{N}(X_i - \bar{X})^2$, where $\hat{Y}_i$ is the fitted value of Y_i from the regression line and $\bar{X}$ is the mean of the true values. The 95% CI for the slope is $\widehat{\beta_1} \pm t_{\alpha=0.025,(N-2)df}\sqrt{\widehat{Var}_{\beta_1}}$.
>
> The absolute value of the estimate of R-squared (R^2) should be > 0.90. The 95% CI for the slope should be completely contained in the interval 0.95 to 1.05.

Repeatability Coefficient (RC): Represents measurement precision where conditions of the measurement procedure (scanner, acquisition parameters, slice locations, image reconstruction, operator, and analysis) are held constant over a "short interval".

Within-subject Coefficient of Variance (wCV): Is often reported for repeatability studies to assess repeatability in test–retest designs. Calculated as seen in the table below:

Steps for Calculating the test-retest wCV

1	Calculate the mean (M) and variance (V) for each of N subjects from their replicate measurements, m1 and m2: $M=(m1+m2)/2;\ V=(m1-m2)^2/2$
2	Calculate the wCV^2 for each of the N subjects by dividing their variance by their mean squared, V/M^2
3	Take the mean of the wCV^2 over the N subjects.
4	Take the square root of the value in step 3 to get an estimate of the wCV.

Appendix D: Platform-Specific Acquisition Parameters for DWI Phantom Scans

For acquisition modalities, reconstruction software and software analysis tools, profile conformance requires meeting the activity specifications and assessment requirements above in Sections 2, 3 and 4.

This Appendix provides specific acquisition parameters, reconstruction parameters and analysis software parameters that are expected to achieve compatibility with profile requirements for technical assessment of MRI systems. Just using these parameters without meeting the requirements specified in the profile is not sufficient to achieve conformance. Conversely, it is possible to use different compatible parameters and still achieve conformance. System operation within provided conformance limits suggests the technical contribution to variance does not unduly alter wCV observed in biological measurements. Technical DWI performance of a given MRI system relative to peer systems can be assessed using the described standardized acquisition protocols designed for existing ice-water DWI phantoms. Platform-specific protocols were excerpted from the QIBA ice water-based DWI Phantom scan procedure for axial acquisitions. The full QIBA DWI Phantom scan procedure involves acquisitions for coronal, axial and sagittal planes as detailed in the QIBA DWI wiki.

Sites using MRI system models listed here are encouraged to consider using parameter settings provided in this Profile for both simplicity and consistency of periodic quantitative DWI QA procedures. Sites using models not listed here may be able to devise their own settings that result in data meeting the requirements of this Profile (at the minimum) or tighter requirements of specific clinical trial.

IMPORTANT: The presence of a product model/version in these tables does not imply it has demonstrated conformance with the QIBA Profile. Refer to the QIBA Conformance Statement for the product.

Table D.1 Model-specific Parameters for Acquisition Devices When Scanning DWI Phantoms

Acquisition Device	Settings Compatible with Conformance		
Philips	*Submitted by: University of Michigan, Department of Radiology*		
	Model / Version	Achieva / 5.1.7	Ingenia / 5.1.7
	Field Strength	1.5T	3T
	Receiver Coil	≥ 8ch head	≥ 15ch head
	Uniformity	CLEAR=yes; Body-Tuned=no	CLEAR = yes
	Slice Orientation	Transaxial	Transaxial
	FOV	220mm	220mm
	Acquisition Voxel Size	1.72x1.72x4 mm	1.72x1.72x4 mm
	Acquisition Matrix†	128x126	128x128
	Recon Voxel Size	0.898x0.898x4 mm	0.898x0.898x4 mm
	Recon Matrix	256x256	256x256
	SENSE (parallel imaging)	Yes, factor=2	Yes, factor=2
	Fold-over Direction	AP	AP
	Fat-shift direction	P	P
	Foldover-sup / Oversampling	No	No
	Qty Slices	25	25
	Stacks and Packages	1	1
	Slice Thickness	4 mm	4 mm
	Slice gap (user-defined)	1 mm	1 mm
	Shim	Volume set to encompass phantom	Vol or PB-Vol to encompass phantom
	B1 shim	Not Applicable	Fixed
	Scan Mode	MS	MS
	Technique	SE	SE
	Acquisition Mode	Cartesian	Cartesian
	Fast Imaging Mode	EPI	EPI
	Shot Mode	Single-shot	Single-shot
	Echoes	1	1
	Partial Echo	No	No
	TE	Shortest (< 125 ms)	Shortest (< 125 ms)
	Flip Angle	90º	90º
	TR	8000 ms	8000 ms
	Halfscan factor	≥ 0.75	≥ 0.75
	Water-Fat shift (in phase dir)	Minimum (~11xAcqVoxel size)	Minimum (~24xAcqVoxel size)
	Fat suppression	No	No
	Diffusion Mode	DWI	DWI
	Direction	“M,P,S” (i.e. non-Overplus)	“M,P,S” (i.e. non-Overplus)
	b-values (user-defined)	0, 500, 1000, 1500, 2000	0, 500, 1000, 1500, 2000
	Average high *b*-values	No	No
	PNS Mode	High	High
	Gradient Mode	Maximum	Maximum
	NSA (averages)	1	1
	Images	M (magnitude)	M (magnitude)
	Preparation phases	Full for 1st scan; Auto for scan 2,3,4	Full for 1st scan; Auto for scan 2,3,4

	EPI 2D Phase Correction	No	No
	Save Raw Data	No	No
	Geometry Correction	Default	Default
	EPI Factor	67	67
	Bandwidth in Freq-direction	1534 Hz	1414 Hz
	Scan Duration	~2 min/scan; 4 scans for ~8 min total	~2 min/scan; 4 scans for ~8 min total

† Matrix size can be 128x128 ± 3

Acquisition Device	Settings Compatible with Conformance		
Siemens	*Submitted by: Siemens Healthcare*		
	Model / Version	Magnetom Aera / VD13	Magnetom Skyra/ VD13
	Field Strength	1.5T	3T
	Receiver Coil	HE1-4	HE1-4
	Slice Orientation	Transaxial	Transaxial
	FOV read and phase	220 mm	220 mm
	Base resolution	130	130
	Phase resolution	100%	100%
	Recon Voxel Size	0.8x0.8x4 mm	0.8x0.8x4 mm
	PAT Mode	GRAPPA, PE factor=2	GRAPPA, PE factor=2
	Phase enc Direction	A → P	A → P
	Ref lines PE	40	40
	Reference scan mode	Separate	Separate
	Qty Slices	25	25
	Phase oversampling	0%	0%
	Slice Thickness	4mm	4mm
	Distance Factor	25%	25%
	Shim mode	Standard	Standard
	Mode	2D	2D
	Multi-slice mode	Interleaved	Interleaved
	EPI factor	130	130
	Free Echo Spacing	Off	Off
	Echo spacing	0.77 ms	0.94 ms
	TE	Minimum (< 125 ms)	Minimum (< 125 ms)
	TR	8000 ms	8000 ms
	Partial Fourier	Off	Off
	Fat suppression	No	No
	Diffusion Mode	Orthogonal	Orthogonal
	Diff. weightings	4	4
	b-value 1,2,3,4	0, 500, 1000, 1500, 2000	0, 500, 1000, 1500, 2000
	Diff. weighted images	On	On
	Trace weighted images	On	On
	Gradient Mode	Fast	Fast
	Averages	1	1
	Averaging mode	Long term	Long term
	Concatenations	1	1
	MTC	Off	Off
	Magn. Preparation	None	None

	Filter	DistortionCorr(2D); PrescanNormalize	DistortionCorr(2D); PrescanNormalize
	Reconstruction	Magnitude	Magnitude
	Bandwidth	1538 Hz/Px	1424 Hz/Px
	RF pulse type	Normal	Normal
	Scan Duration	~2 min/scan; 4 scans for ~8 min total	~2 min/scan; 4 scans for ~8 min total

Acquisition Device	Settings Compatible with Conformance		
General Electric	*Submitted by: Memorial Sloan Kettering Cancer Center; and GE Healthcare*		
	Model / Version	Optima MR 450 / DV23.1	Discovery MR 750 / DV23.1
	Field Strength	1.5T	3T
	Receiver Coil	8HRBrain	8HRBrain
	Slice Orientation	Transaxial	Transaxial
	FOV	22 cm	22 cm
	Phase FOV	100%	100%
	Acquisition matrix	128x128	128x128
	Acq voxel size	1.72x1.72x4 mm	1.72x1.72x4 mm
	Recon voxel size	0.98x0.98x4 mm	0.98x0.98x4 mm
	ASSET Acceleration, Phase	2	2
	Freq enc. Direction	R/L	R/L
	Qty Slices	25	25
	Slice Thickness	4 mm	4 mm
	Slice spacing	1 mm	1 mm
	Shim	Auto	Auto
	Imaging Options	2D, spin-echo, EPI, DIFF	2D, spin-echo, EPI, DIFF
	Num Shots	1	1
	Dual Spin Echo	No	No
	TE	Minimum (<125 ms)	Minimum (<125 ms)
	TR	8000 ms	8000 ms
	Partial Fourier	OFF	OFF
	Fat suppression	No	No
	Diffusion Direction	ALL	ALL
	b-value	0, 500, 1000, 1500, 2000	0, 500, 1000, 1500, 2000
	Phase Correct	On	On
	dB/dt control mode	1st	1st
	NEX	1	1
	Bandwidth	Default (250 kHz)	Default (250 kHz)
	3D Geometry correction	No	No
	Scan Duration	~2 min/scan; 4 scans for ~8 min total	~2 min/scan; 4 scans for ~8 min total

Acquisition Device	Settings Compatible with Conformance			
Canon	*Submitted by: Canon Medical Systems*			
	Model/Version	Elan / 6.0SP1061	Orian / 8.0SP0041	Galan / 8.0SP0041
	Field Strength	1.5T	1.5T	3T
	Receiver Coil	Octave head/neck coil	16 head/neck coil	16 or 32-ch head/neck coil
	Slice Orientation	Transaxial	Transaxial	Transaxial
	FOV	22 cm x 22 cm	22 cm x 22 cm	22 cm x 22 cm
	Matrix Size	128 x 128	128 x 128	128 x 128
	No Wrap	1	1	1
	SPEEDER Acceleration, Phase	2	2	2
	Phase Encode	AP	AP	AP
	Number of TE-echoes	16	16	16
	Qty Slices	25	25	25
	Slice Thickness	4 mm	4 mm	4 mm
	Slice Spacing	1 mm	1 mm	1 mm
	Sequence	SEEPI2D	SEEPI2D	SEEPI2D
	Number of Shots	1	1	1
	Segmentation Type	Sequential	Sequential	Sequential
	TE	Minimum (< 125 ms)	Minimum (< 125 ms)	Minimum (< 125 ms)
	TR	8000 ms	8000 ms	8000 ms
	Fat Suppression	Off	Off	Off
	Diffusion Direction	3-axis mixed	3-axis mixed	3-axis mixed
	b-value	0, 500, 1000, 1500, 2000	0, 500, 1000, 1500, 2000	0, 500, 1000, 1500, 2000
	Phase Correction	Type 2 (EPI Nyquist Ghosting)	Type 2 (EPI Nyquist Ghosting)	Type 2 (EPI Nyquist Ghosting)
	NAQ	1	1	1
	Receiver Bandwidth	1563 Hz / pixel	1563 Hz / pixel	1421 Hz / pixel
	RF Type	Normal	Normal	Normal
	GR Type	Fast	Fast	Fast
	Scan Duration	~2 min/scan	~2 min/scan	~2 min/scan

Appendix E: Technical System Performance Evaluation

Procedures below are for basic evaluation of MRI equipment performance to qualify for quantitative DWI trials. Conformance specs for performance metrics (listed in 3.2.2) are suggested to ensure that technical measurement errors related to the MRI system do not unduly contribute to measurement variance for subject ADC.

E.1. ADC Qualities at/near Isocenter

To evaluate an MRI system for ADC measurement bias and precision, a phantom containing media having known diffusion properties is required. Water maintained at 0 ˚C is widely used as a known standard with diffusion coefficient = 1.10×10^{-3} mm^2/s and is the basis for ice water-based DWI phantoms [61, 62, 65, 115]. Scanners should image phantoms in the axial/transverse plane, and cylindrical geometries should align with the main magnetic field direction.

This procedure requires access to an ice water DWI phantom, such as the QIBA DWI phantom [63, 64, 67] or alternative that contains a measurement sample of water (≥ 30 mL volume) located at isocenter surrounded by an ice water bath [61, 62, 65, 115]. Sufficient time must be allowed for the sample to achieve thermal equilibrium (≥ 1 hour) and the phantom must contain an adequate volume of ice to surround the measurement sample over the entire MRI exam period. Details for preparation and use of the QIBA DWI phantom are available in the QIBA DWI wiki. The phantom ADC measurement protocol should follow the DWI scan parameters defined in Appendix D, Table D.1, which involves DWI acquisition at nominal *b*-values = 0, 500, 1000, 1500, 2000 s/mm^2.

Typically, MRI systems exhibit best performance at or near isocenter where ADC bias reflects overall calibration of gradient amplitude and DWI sequence timing. Proximity to isocenter is to be determined by location of the center of an ROI used to assess ADC. Spatial coordinates of the ROI-center are often available using the scanner's electronic caliper read-out of ROI-center coordinates in the patient-based frame of reference defined by "Patient Landmark" location. Note, the patient-based frame and magnet-based frame (true isocenter) may not be synonymous, and displacement between the two may vary from scan series to scan series. To maintain minimal offset between patient-based and magnet-based frames, the "Patient Landmark" should be defined on the center of the phantom then the prescription of slices used for quantitative evaluation should be kept centered on Superior/Inferior=0 mm (for horizontal bore magnets). An ROI having center coordinates [*RL, AP, SI*] is "at isocenter" when $\sqrt{RL^2 + AP^2 + SI^2} \leq 4\,cm$, and the maximum diameter of the ROI ≤ 2 cm. A minimum ROI diameter of ~1 cm will provide a sufficient number of pixels (> 80) for adequate sampling of phantom ADC heterogeneity for reliable estimate of within ROI statistics (standard deviation and mean). For uniform analysis, "QibaPhanR1.4" software provided through the QIDW (https://tinyurl.com/DWIPhantomResources) can be used to generate the relevant ADC ROI assessment metrics (bias, precision, repeatability and SNR) for QIBA DWI phantom, as described below.

The QIBA DWI phantom, and other water-based phantoms are isotropic so measured diffusion coefficient ***should*** be independent of applied diffusion gradient direction. Throughout this profile and assessment procedure, "DWI" will refer to the composite of three orthogonal DWIs as the trace DWI.

Two or more diffusion weightings are required to calculate ADC, and full ADC maps are generated on a pixel-by-pixel basis (though low SNR may bias these pixel-by-pixel ADC maps) using the mono-exponential model:

$$ADC_{bmin,b} = \frac{1}{(b-bmin)} \ln\left[\frac{S_{bmin}}{S_b}\right], \qquad \text{EQ(1)}$$

where S represents the diffusion weighted image intensity and subscripts refer to *b*-value. For this assessment procedure, if only two *b*-values are used, they must include the nominal minimum *b*-value in the calculation, typically *b*=0. If all *b*-values are used in the ADC calculation, a mono-exponential signal decay versus *b*-value model fit (e.g., least-squares) must be used. To achieve adequate diffusion contrast for ADC estimation via EQ(1), $(b - b_{min})$ should be ≥ 400 s/mm^2.

The estimate of MRI system ADC bias in measurement of 0°C water (DC_{true} = 1.1x10^{-3} mm^2/s [61]) at isocenter should be calculated as:

$$ADC\ bias\ estimate = \mu - DC_{true};\ \ or\ \%bias = \frac{100\%\,(\mu - DC_{true})}{DC_{true}}, \qquad \text{EQ(2)}$$

where μ is the ROI mean of the ADC map at isocenter and the ROI contains 80-150 pixels. Assuming the pixel values follow a normal distribution, the 95% confidence interval (CI) for this bias estimate is,

$$ADC\ bias\ estimate\ \pm 1.96\ \frac{\sigma}{\sqrt{N}}, \qquad \text{EQ(3)}$$

where σ is the standard deviation of ADC pixel values in the ROI containing *N* pixels. ADC bias at isocenter allowed by this profile is |ADC bias| ≤ 0.04x10^{-3} mm^2/s.

The standard deviation of ADC pixel values within an isocenter ROI is one indicator of random measurement error (precision) in ADC maps expressed as a percentage relative to the ROI mean (%CV) as:

$$ADC\ error\ estimate = 100\ \cdot\ \frac{\sigma}{\mu} \qquad \text{EQ(4)}$$

Similar to ADC bias estimate, this procedure typically uses an ROI of ~1 cm^2 (> 80 pixels) on a water sample at 0 ºC (e.g., center tube of QIBA DWI phantom) at isocenter, and follow the QIBA DWI phantom scan protocol to estimate ADC error. The random error allowed by this profile specs (3.2.2) is < 2%.

The established QIBA DWI phantom scan protocol is to acquire four DWI scans (each ~2 minutes) in immediate succession holding acquisition conditions constant. This procedure serves multiple aims: (1) inspect for monotonic trend in ADC vs. time suggesting the phantom was not at thermal equilibrium; (2) inspect for artifact or drift suggesting system instability; (3) allow for estimation of voxel signal-to-noise ratio (SNR); and (4) provide an estimate of short-term (intra-exam) repeatability [61, 64-67]. Repeated scanning of the phantom over multiple days/weeks/months more closely resembles serial scanning of patients in longitudinal studies. Regardless of interval over which repeated measurements are performed, assuming normally distributed measures, the Repeatability Coefficient (RC) and "within-subject" Coefficient of Variation as a percentage (wCV) are calculated as [30, 35, 36]:

$$RC = 2.77\ \cdot\ \sigma_w; \quad wCV = \ 100\ \frac{\sigma_w}{\mu}\ , \qquad \text{EQ(5)}$$

where σ_w^2 is the within-subject (phantom) parameter variance (see Appendix C for calculation of the wCV) and μ is the parameter mean. The average of repeated ROI means at isocenter and square root of variance of these means may be used in EQ(5) to estimate *RC* and *wCV* as a metric of system technical performance. The allowed short-term and long-term ADC repeatability for this profile are ≤ 1.5 x 10^{-5} mm^2/s and ≤ 6.5 x 10^{-5} mm^2/s, respectively [65], which are necessary for assessment of the impact of SNR. For long-term reproducibility, it is key to consistently position the phantom in the same orientation. Please note, phantom-based *RC* and *wCV* derived here are under relatively ideal conditions and should not be taken as representative of repeatability achieved in human DWI/ADC studies, which involve more sources of variability. Section 3.2.2 summarizes the acceptable baseline performance for the device assessed with the quantitative DWI phantom and required by this profile to ensure no significant contribution to the within-subject RC and CV.

For studies involving off-isocenter ADC measurements (adjusted for orientation), the maximum ADC bias in a cylindrical volume with a 4 cm radius and a 20 cm length, centered around a point between 8–12 cm off-isocenter, shall be less than 10%.

E.2. DWI Signal to Noise

This section describes criteria that are necessary for an MRI system to meet the Profile qualification specs listed in 3.2.2. Vendors and imaging sites can use this procedure to estimate relative signal-to-noise ratio (SNR) of an MRI system in the context of DWI and parametric ADC maps (both for phantom and subjects).

SNR of any MR image is heavily dependent on acquisition conditions. While SNR is informative of system performance, its evaluation by the suggested procedure is not an absolute system performance metric.

Determination of SNR by this procedure serves two aims: (1) provide a relative system performance metric; (2) confirm SNR was adequate to assess ADC bias without incremental bias due to low SNR.

This procedure is used to estimate SNR at the acquisition voxel level. Common filtering, interpolation, and reconstruction algorithms lead to correlated noise in neighboring DWI pixels. Therefore, the described procedure relies on analysis that yields a noise estimate averaged over an ROI to mitigate correlated noise.

Signal estimated as the mean pixel intensity value over an ROI is straightforward; however, DWI noise estimation is more difficult. Using standard deviation of pixel values in signal-free background (i.e., air) as a noise estimate is unreliable due to commonly-used parallel imaging reconstruction, coil-sensitivity equalization routines, and Rician bias of "magnitude" signals [93-95, 116, 117, 119]. Instead, for this procedure, noise will be estimated by the temporal change in pixel values measured over multiple scans. The QIBA DWI phantom scan protocol requires four scans repeated in immediate succession, holding all acquisition conditions constant. Images containing the measurement ROI over these four dynamics should be visually inspected for conspicuous (multipixel) spatial shift, distortion, or artifact in any of the dynamics. Assuming none, random noise is considered to be the main contributor to scan-to-scan differences. To assess noise by this procedure, software (e.g., QibaPhanR1.4) must be available to combine dynamic images and calculate the temporal standard deviation of each pixel (i.e., over the "n" dynamic scans). An image comprised of the temporal standard deviation of pixel values should be referred to as the "temporal noise image". An image comprised of the temporal mean of pixel values should be referred to as the "signal image". Note, an image comprised of the pixel-by-pixel division of the signal image by the temporal noise image is referred to as the "signal-to-fluctuation-noise-ratio image" [118, 119], but this should not be used to estimate SNR. Instead, the calculation estimates noise as spatial mean within an ROI of temporal noise image and corresponding signal as a spatial ROI mean of the temporal average signal image [117]:

$$SNR_{nDyn} = \frac{Spatial\ mean\ pixel\ value\ \ on\ Signal\ Image}{Spatial\ mean\ pixel\ value\ on\ Temporal\ Noise\ Image} \qquad \text{EQ(6)}$$

The 95% confidence interval for this SNR estimate is $\pm 1.96\ \frac{\sigma_{SNR}}{\sqrt{N}}$,

where $\sigma_{SNR} = SNR_{nDyn}\sqrt{sCV^2 + nCV^2}$ is the "error propagation" estimate of standard deviation of SNR pixel values in an ROI containing N pixels with spatial coefficients of variance, sCV and nCV, for the temporal average signal image and temporal standard-deviation noise image, respectively.

An alternative procedure to estimate SNR from an even quantity of dynamic scans is to first sum all odd-numbered dynamics called "sumODD image" and sum all even-numbered dynamics called "sumEVEN image", then create their difference: "DIFF image" = sumODD – sumEVEN. Using these, an estimate of SNR within an ROI from n-dynamic scans acquired in immediate succession holding conditions fixed should be calculated as [118, 119]:

$$altSNR_{nDyn} = \sqrt{n}\ \frac{Spatial\ mean\ pixel\ value\ on\ Signal\ Image}{Spatial\ standard\ deviation\ pixel\ value\ on\ DIFF\ Image}\ . \qquad \text{EQ(7)}$$

EQ(7) should be used when only two dynamic scans (n=2) are available.

For conditions defined in this assessment procedure (i.e. 4 dynamics and 80-100 pixel ROIs) equation EQ(6) tends to overestimate SNR slightly although has tighter confidence interval relative to equation EQ(7). The choice of which equation to use may depend on capabilities of the analysis software. SNR analysis via equations EQ(6) and/or EQ(7) may be performed on source DWI images, as well as on derived ADC maps.

In situations where two or more dynamic series are not available, the "noise" level may be crudely estimated (i.e. still subject to Rician bias and background regularization) by the standard deviation in signal-free background or by the standard deviation within the ROI defined on uniform signal-producing area. Prior to defining the background ROI, the assessor should inspect the images with a tight window/level and strive to select a background region that contains uniform random noise while avoiding signal gradients, structured noise (e.g., ghosts) or severely modulated zones (often masked to "zero"). While considered unreliable for reasons stated above, the equation to estimate SNR of an ROI in signal-producing region relative to background region is:

$$SNR_{vs\ bkgnd} = \frac{Spatial\ mean\ pixel\ value\ on\ Signal\ Image}{Spatial\ standard\ deviation\ pixel\ value\ in\ background\ ROI}. \qquad \text{EQ(8)}$$

Since performed on magnitude images, this procedure under-estimates noise thus over-estimates SNR. This Rician bias may be predicted using DWI DRO and could be appropriately factored into further analysis of ADC statistics [93, 94, 117].

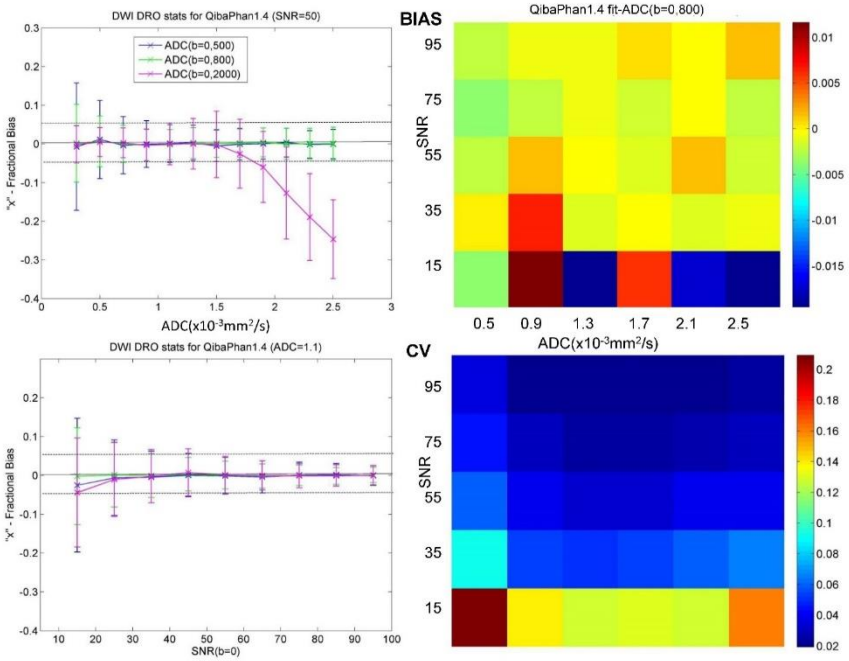

Figure E.1**:** Examples of fractional-bias and CV metrics for DWI-DRO ADC maps generated using QibaPhan1.4 SW. Left panes show fractional ADC bias and SD (error-bars) as a function of true (i.e., DRO input) ADC (top: at SNR=50) and SNR (bottom: at ADC=1.1 x 10^{-3} mm^2/s) for three *b*-values (color-coded in legend). The dotted horizontal lines mark ± 5% deviation to guide optimal DWI parameter ranges for ADC, SNR, *b*-value. Mean bias appears to be dependent on ADC and *b*-value and independent of SNR, while bias SD closely follows CV-trend and mostly SNR-dependent. Right panes show the SNR/ADC maps for mean bias and CV metrics at *b*-value=800 (typical of liver DWI protocol), indicating that the fit-ADC bias error (mean +/- SD) falls within +/-5% for SNR >50 in liver ADC range (0.7–1.7) x 10^{-3} mm^2/s.

At a minimum, the evaluation procedure outlined in EQ(6) and EQ(7) should be performed on the *b*=0 diffusion weighted image. Low SNR conditions can introduce bias in ADC measurement (see Figure E.1). To satisfy site qualification requirements (3.2.2) and avoid introduction of bias due to low SNR conditions, an MRI system should have SNR ≥ 50 □ 5 for the *b*=0 image in an ROI of 1 cm diameter (80–100 pixels). This SNR will allow measurement of mono-exponential diffusion media having diffusion coefficients ≤ 1.1x10^{-3} mm^2/s (e.g., water at 0 ^oC) using *b*-values ≤ 2000 s/mm^2 and avoid incremental bias due to noise. SNR limits for different ADC and *b*-value ranges relevant for clinical trials should be assessed using the DWI DRO provided through the QIDW (e.g., Figure E.1).

E.3. ADC *B*-VALUE DEPENDENCE

The QIBA DWI phantom and other ice water phantoms ***should*** exhibit mono-exponential signal decay with increasing *b*-value. Any apparent change in measured ADC with choice of *b*-value suggests one or combination of the following: (1) output gradient amplitude is not linear with input demand; (2) background

gradients that have substantial but variable contribution to the actual *b*-value; (3) spurious signal in $b \approx 0$ DWI that is eliminated at moderately low *b*-values (e.g., $b \geq 50$ s/mm^2); and (4) inadequate SNR at high *b*-values. To evaluate whether an MRI system exhibits artifactual *b*-value dependence in ADC measurement, ADC values measured at isocenter on an ice water phantom should be compared as a function of *b*-value pairs described in equation 1. The lowest *b*-value (typically $b_{min} = 0$) must be included in each *b*-value pair. The assessor should calculate *b*-value dependence as:

$$ADC\ bvalue\ dependence = 100\% \left\| \frac{(ADC_{bmin,b2} - ADC_{bmin,b1})}{ADC_{bmin,b1}} \right\|, \qquad \text{EQ(9)}$$

where $b_2 \neq b_1$. Note, adequate diffusion contrast is required for ADC estimation via EQ(1), therefore both $(b_1 - b_{min})$ and $(b_2 - b_{min})$ should be ≥ 400 s/mm^2. The allowed *b*-value dependence that would not significantly influence the claims of this profile, is < 2% (3.2.2).

In the absence of a phantom with varying ADC with known ground truths, this *b*-value dependence assessment provides a suitable test for ADC linearity.

E.4. ADC Spatial Dependence

All ADC calculations described above utilize nominal *b*-values entered by the assessor during DWI acquisition and retained in DICOM headers. In turn, *b*-value selection determines amplitude and timing of diffusion-encoding gradient pulses within the diffusion sequence. Due to current physical constraints of gradient designs, gradient strength is not spatially uniform throughout the imaged volume. The greatest contributor to spatial ADC bias is gradient nonlinearity, although other sources such as uniformity of the main magnetic field can also contribute to spatial ADC bias at off-center locations [62, 66, 120-124]. Regardless of source, the maximum level of allowable spatial ADC bias of an MRI system depends on scale of the imaging volume for the specific clinical application. For example, DWI studies dedicated to the prostate or brain lesions could benefit from relatively minimal expected spatial ADC bias when the imaging prescription requires the lesion be located near superior/inferior = 0 mm; whereas bilateral breast or unilateral off-center liver DWI will likely experience greater spatial ADC bias. For MRI system performance evaluation, a DWI phantom should be selected that reasonably spans the imaging volume of the associated clinical application and that preferably fits in the same application-specific receiver coil. By its physical nature (determined by gradient coil design), spatial ADC bias is expected to be independent of *b*-value and ADC range. Thus, assessment of this bias for phantom is a reasonable estimate for bias in patient scans in clinical trials. In the context of clinical trial, spatial ADC bias is expected to increase both the ROI ADC error (i.e., in ROI mean and ADC histogram width, and increasing wCV), and the variability among systems.

Using DWI phantom with known diffusion coefficient, such as the QIBA DWI phantom or other suitable ice water-based phantom, the site should follow established phantom preparation instructions, and acquire DWI using a protocol matched to the associated application. Using EQ(2), ADC bias should be measured from multiple ROIs containing at least 80 pixels each that reasonably sample spatial offset(s) from magnet isocenter anticipated for the specific clinical application. Maximum allowed bias for a system qualified for this profile (3.2.2) will increase with maximum allowed offset from isocenter (4% for 4 cm AP/RL/SI, 10% for RL/AP 4–10 cm (SI < 4 cm) or SI 4–10 cm (RL/AP < 4 cm)).

Appendix F: Checklists

F.1. Site Checklist

Parameter	Conforms (Y/N)	Requirement
Site Qualification (Section 3.2)		
Qualification activities	□ Yes □ No	Shall perform qualification activities for Acquisition Device, Scanner Operator, and Image Analyst to meet equipment, reconstruction SW, image analysis tool and phantom ADC performance metrics as specified in Table 3.2.2 and by trial-specific protocol 3.6.2
Periodic QA (Section 3.5)		
Periodic DWI QA	□ Yes □ No	Shall perform annual periodic QA (and after major hardware or software changes) for Acquisition Device that includes assessment of ADC bias, random error, linearity, DWI SNR, DWI image artifacts, *b*-value dependence (linearity) and spatial uniformity (3.2.2)
Equipment	□ Yes □ No	Same, pre-qualified equipment and SW shall be used over the length of trial, and all preventive maintenance shall be documented over the course of the trial. Re-qualification shall be performed in case of major SW or hardware upgrade. Study of each patient shall be performed on the site pre-qualified scanner using approved receiver coil and pre-built profile-conformant scan protocol (3.6)

F.2. Acquisition Device Checklist

Parameter	Conforms (Y/N)	Requirement
Site Qualification (Section 3.2)		
DWI Tags	□ Yes □ No	Shall preserve tags related to DWI, including private tags, which may be vendor-specific. Some key tags are specified in Appendix D.
Short-term (intra-exam) ADC repeatability at/near isocenter	□ Yes □ No	RC $\leq 1.5 \times 10^{-5}$ mm^2/s and wCV $\leq 0.5\%$ for ice-water phantom or other quantitative DWI phantom
Long-term (multi-day) ADC repeatability at/near isocenter	□ Yes □ No	RC $\leq 6.5 \times 10^{-5}$ mm^2/s and wCV $\leq 2.2\%$ for ice-water phantom or other quantitative DWI phantom
DWI *b*=0 SNR	□ Yes □ No	SNR (b=0) $\geq 50 \pm 5$ for ice-water phantom or other quantitative DWI phantom.
ADC *b*-value dependence	□ Yes □ No	< 2% for ice-water phantom or other quantitative DWI phantom over *b*-value pairs 0-500; 0-1000; 0-1500; and 0-2000 s/mm^2
Maximum |bias| within 4 cm of isocenter	□ Yes □ No	< 4% for uniform known ADCs within DWI phantom

Parameter	Conforms (Y/N)	Requirement
ADC error at/near isocenter	□ Yes □ No	ADC random error ≤ 2% for ice-water phantom or other quantitative DWI phantom
Optional: Additional requirements for studies involving off-center ADC measurement:		
R/L offset 4–10 cm (A/P and S/I < 4 cm)	□ Yes □ No	< 10% for uniform known ADCs within DWI phantom
A/P offset 4–10 cm (R/L and S/I < 4 cm)	□ Yes □ No	< 10% for uniform known ADCs within DWI phantom
S/I offset 4–10 cm (R/L and A/P < 4 cm)	□ Yes □ No	< 10% for uniform known ADCs within DWI phantom
Protocol Design (Section 3.6)		
Scan Protocol Parameters, DICOM Conformance, and Image Reconstruction	□ Yes □ No	Device scan protocol parameters shall be within organ-specific ranges listed in the protocol specification tables (3.6.2). Shall be capable of performing reconstructions and producing images with all the parameters set as specified. Shall meet DICOM header and image registration requirements specified in 3.10.2, including storage of *b*-values, DWI directionality, image scaling and units tags, as specified in DICOM conformance statement for the given scanner SW version, as well as the model-specific Reconstruction Software parameters utilized to achieve conformance.
Image Distribution (Section 3.12)		
Image DICOM	□ Yes □ No	DICOM tags essential for downstream review and diffusion analysis shall be maintained including pixel intensity scaling [114], *b*-value, and DWI directionality vs. trace, and ADC scale and units. Trace DWI DICOM at each *b*-value shall be archived in the local PACS.

F.3. SCANNER OPERATOR CHECKLIST

Parameter	Conforms (Y/N)	Requirement
Site Qualification (section 3.2)		
Acquisition Protocols	□ Yes □ No	Shall prepare scan protocols conformant with section 3.6.2 "Protocol Design Specification" and phantom qualification (Appendix D) and ensure that DWI acquisition parameters (*b*-value, diffusion direction) shall be preserved in DICOM and shall be within ranges allowed by study protocol (both for phantom and subject scans). Shall check for protocol conformance, consistent patient positioning (orientation, target lesion location relative to isocenter), and that all subject-specific adjustments (i.e., to suit body habitus) are consistent across serial scans.
Acquisition Device Performance	□ Yes □ No	Shall perform assessment procedures (Section 4) for site qualification and longitudinal QA for the acquisition devices participating in trial to

Parameter	Conforms (Y/N)	Requirement
		document acceptable performance for phantom ADC metrics as specified in table 3.2.2
Acquisition Device	□ Yes □ No	The same scanner shall be used for baseline and subsequent longitudinal measurements for detecting change in ADC.†
Image Data Reconstruction (section 3.10)		
Trace DWI and ADC map generation across subjects and time	□ Yes □ No	Number and magnitude of *b*-values shall be consistent across TPs for patients. ADC maps shall be generated in a consistent manner across TPs, including post-processing, fit model, and image registration.
b-value record	□ Yes □ No	Scanner operator shall verify that the reconstruction SW records *b*-values, or if not shall manually record the *b*-values, that are used to generate the ADC map.
ADC maps	□ Yes □ No	ADC maps shall be preserved with DICOM scale tags. ADC map scale/units and *b*-values used for generation shall be recorded.

† Not using the same scanner and image acquisition parameters for baseline and subsequent measurements does not preclude clinical use of the measurement but will exclude meeting the requirements of the Profile claim.

F.4. IMAGE ANALYST CHECKLIST

Parameter	Conforms (Y/N)	Requirement
Staff Qualification (section 3.1)		
Qualification	□ Yes □ No	Shall be a radiologist, technologist, physicist, or other scientist with documented and authorized training in terms of: anatomical location and image contrast(s) used to select measurement target; understanding key principles of diffusion weighting, directionality, and diffusion test procedures; procedures to maintain diffusion-related DICOM metadata content along the network chain from Scanner to PACS and analysis workstation; the use of the Image Analysis Tool, including ADC map generation from DWI (if not generated on the scanner), and ADC map reduction to statistics with ROI/VOI location(s)
Site Qualification (section 3.2)		
Image Analysis Tool Performance	□ Yes □ No	Shall test Image Analysis Tool to ensure acceptable performance according to 3.13.2 specifications for study image visualization, DICOM and analysis meta-data interpretation and storage, ROI segmentation, and generation of ADC maps and repeatability statistics for qualification phantom (below)
Phantom ADC ROI	□ Yes □ No	Shall confirm that phantom ADC ROI is 1–2 cm diameter (> 80 pixels without interpolation) for all Acquisition Device specifications in Table 3.2.2

Parameter	Conforms (Y/N)	Requirement
Phantom ADC metrics	□ Yes □ No	Shall evaluate and record phantom ADC metrics (bias, linearity and precision) according to Table 3.2.2 specifications for Acquisition Device qualification and periodic QA using QIBA-provided or qualified site Image Analysis Tool, or QIBA-certified 3rd party analysis services
Image Analysis (section 3.13)		
ROI Determination	□ Yes □ No	Shall segment the ROI on ADC maps consistently across time points using the same software / analysis package guided by a fixed set of image contrasts and avoiding artifacts

F.5. RECONSTRUCTION SOFTWARE

Parameter	Conforms (Y/N)	Requirement
Image Data Reconstruction (Section 3.10)		
Trace DWI	□ Yes □ No	Trace DWI shall be auto-generated on the scanner and retained for all $b > 0$. For equal b-value on 3 orthogonal directions, trace DWI is the geometric average of the 3-orthogonal directional DWI.

F.6. IMAGE ANALYSIS TOOL CHECKLIST

Parameter	Conforms (Y/N)	Requirement
Image Analysis (section 3.13)		
ROI geometry	□ Yes □ No	Screenshot(s) documenting ROI placement on ADC maps shall be retained in the subject database for future reference ROI as a binary pixel mask in image coordinates is desired in the subject database for future reference. Ideally, ROI shall be saved as a DICOM segment object
Image Display	□ Yes □ No	Software shall allow operator-defined ROI analysis of DWI/ADC aided by inspection of ancillary MR contrasts Ideally, above plus multi view-port display where DWI/ADC and ancillary MR contrasts from the same scan date are displayed side-by-side and geometrically linked per DICOM (e.g., cursor; crosshair; ROI; automatically replicated in all view-ports); ROIs/VOIs may include multiple noncontiguous areas on one slice and/or over multiple slices
Analysis Procedure	□ Yes □ No	Analysis steps, derived metrics and analysis software package shall be held constant for all subjects and serial time points

Parameter	Conforms (Y/N)	Requirement
ADC statistics	□ Yes □ No	Shall allow display and retention of ROI statistics in patient DICOM database (PACS). Statistics shall include ADC mean, standard deviation, and ROI/VOI area/volume Ideally, ADC pixel histogram, additional statistics for ADC maximum, minimum, exclusion of "NaNs", and explicit recording of inclusion or exclusion of "zero-valued pixels shall be retained with the statistics
Fit algorithm type	□ Yes □ No	The specific choice of the fit algorithm (e.g., linear fit to logarithmic SI vs. non-linear fit with Rician noise, a particular scanner software version, etc.) shall be recorded, held constant within a study and reported with any dissemination of study findings.
Fit algorithm bias	□ Yes □ No	For offline ADC map generation, the mean ADC shall agree with scanner-generated, or DRO ground truth, ADC values to within one ROI standard deviation.
b-value and direction	□ Yes □ No	Software shall extract *b*-values and diffusion axis direction from DICOM header
Phantom ADC QC metrics	□ Yes □ No	Software with independent QA option shall evaluate and report phantom scan protocol compliance and ADC metrics including bias, random error, linearity, DWI SNR, *b*-value dependence, and spatial uniformity according to Table 3.2.2 to enable performance assessment for Site qualification (3.2) and periodic QA (3.5)